International Tables for Crystallography (2018). Vol. H, Chapter 2.7, pp. 156–173.

2.7. High-pressure devices

A. Katrusiak

2.7.1. Introduction

Although life in the biosphere of Earth exists within narrow limits of temperature and pressure, these thermodynamic conditions are unusual *on* Earth and in the Universe. Most of the matter in the Universe is contained in black holes, stars and planets, where it is exposed to extreme temperature and pressure. On the other hand, interstellar space constitutes most of the Universe's volume, where both pressure and temperature are close to their absolute-zero values. On Earth's surface at sea level, atmospheric pressure is about 1000 hPa [1 atm = kG cm^{-2} = 9.807 $\times$ 10^4 Pa $\simeq$ 0.1 MPa; currently, the pascal (abbreviated Pa) is the generally accepted pressure unit recommended by the International System of Units]. Under water on Earth, the pressure increases by 0.1 MPa for every 10 m depth, and rises to 120 MPa at the bottom of the Mariana Trench, 11 km below the sea's surface. A relatively low pressure change, to about 0.3 MPa at a depth of 20 m, affects the dissolution of nitrogen in human blood and can lead to decompression sickness (caisson disease); at 300 m in the oceans (3 MPa) and 288 K, methane forms stable hydrates, which constitute the most abundant deposits of carbon on Earth. All geological deposits are exposed to some pressure; at a depth of 1000 m this is about 300 MPa. Consequently, the structure and properties of very many minerals, formed and deposited in the crust, can transform considerably after their exposure to the surface. The syntheses of numerous minerals require high-pressure conditions. Thus, high-pressure experiments can provide indispensable information about the geological and stellar mechanisms, transformations and properties governing the matter forms, properties and distribution inside stars and planets.

Therefore, the pressure dependence of crystal structures is of primary interest to geologists, planetologists and astrophysicists (Hazen, 1999; Merlini *et al.*, 2012). The most cited examples of the effects of extreme conditions are thermonuclear synthesis, the formation of diamond (the dielectric carbon allotrope), the formation of stishovite (the dense form of SiO_2) and the propagation of seismic waves through the Earth's crust. The understanding of these and other phenomena requires that extreme conditions be reproduced and crystal structures investigated in laboratories. Most importantly, the conditions that are ubiquitous across the Universe are viewed as extreme only from our perspective of a narrow thermodynamic space, of a few tens of kelvin and a few megapascals around the triple point of water. From this narrow thermodynamic space, most of our knowledge of materials science has been developed. Extreme conditions allow theories to be verified and developed to a more general level. Moreover, extreme conditions can be utilized to produce new materials with desired properties (Hanfland *et al.*, 2011; Senyshyn *et al.*, 2009), including diamond or its other super-hard substitutes, or new forms of pharmaceutical drugs (Boldyreva, 2010; Boldyreva *et al.*, 2002, 2006; Fabbiani, 2010; Fabbiani & Pulham, 2006; Fabbiani *et al.*, 2004, 2005, 2009). The key element for such research is a sample-environment device for generating high pressure in the laboratory.

The pressure at the centre of Earth is about 364 GPa, one order of magnitude higher again inside the giant planets Jupiter and Saturn, and over 1 000 000 GPa (*i.e.* 1000 TPa) inside small stars like the Sun. Structural determinations under varied thermodynamic conditions are essential for the general understanding of physical and chemical phenomena, and to gain knowledge about the properties of materials and to describe the world around us. Indeed, the biosphere where we live is confined to a range from 0.33 atm (0.033 MPa) at the top of Chomolungma (Mt Everest), 8848 m above sea level, to about 1200 atm (120 MPa). The most commonly discussed and studied thermodynamic parameters are temperature (T), pressure (P) and composition (X). In principle, they affect the structure of matter differently. For example, the primary change induced by temperature is in the energy of atomic, molecular and lattice vibrations, whereas increasing pressure always reduces the volume. These changes are interdependent, and the compression of a structure can also reduce its thermal vibrations, change the types of cohesion forces and reverse the balance between competing compounds of different composition. This concerns all compounds, not only minerals deep under the Earth's surface. An exciting example of a molecular compound undergoing such transformations is water, transforming between at least ten polymorphic structures at high pressure, and also forming hydrates, depending on the thermodynamic conditions. Hence, pressure is now utilized to generate new polymorphs and solvates that cannot be obtained under normal conditions (Patyk *et al.*, 2012; Tomkowiak *et al.*, 2013; Fabbiani, 2010; Boldyreva, 2010).

For these reasons, high-pressure techniques have been developed dynamically, and the breakthrough invention of the diamond-anvil cell and its development in the second half of the 20th century greatly intensified high-pressure research. Today, the effects of high pressure on various materials and their reactions are studied both in small laboratories in universities and at large facilities, which provide powerful beams of X-rays from synchrotrons and beams of neutrons from reactors and spallation targets. The large facilities are either international initiatives, like the European Synchrotron Radiation Facility (ESRF) and Institute Laue–Langevin (ILL) in Grenoble, France, or national ones, like the Diamond Light Source and ISIS at the Rutherford Appleton Laboratory in Oxfordshire, UK, the Deutsches Elektronen Synchrotron (DESY) in Hamburg, Germany, the Photon Factory in Tsukuba, SPring-8 (Super Photon ring – 8 GeV) in Hyōgo Prefecture and the Japan Proton Accelerator Research Complex (J-PARC) in Tokal near Tokyo, Japan, the National Synchrotron Light Source (NSLS) at Brookhaven National Laboratory, USA, the Advanced Photon Source (APS) at Argonne National Laboratory and Los Alamos National Laboratory (LANL), New Mexico, USA, the Lawrence Livermore National Laboratory, California, USA, the Joint Institute for Nuclear Research (JINR) in Dubna, Russian Federation, the Spallation Neutron Source (SNS) at Oak Ridge National Laboratory, USA, and others. They provide access to the beams and high-pressure equipment to the general scientific community.

2.7.2. Historical perspective

The earliest concepts of pressure are often associated with Evangelista Torricelli's famous statement '*Noi viviamo sommersi nel fondo d'un pelago d'aria*' ('We live submerged at the bottom

of an ocean of air') in 1643, Otto von Guericke's experiment pitting the force of six horses against atmospheric pressure acting to squeeze together two hemispheres evacuated using the vacuum pump he had constructed in Magdeburg in 1654, and Blaise Pascal's measurements of pressure differences at different altitudes and his demonstrations of barrels being blown up by the force of water poured in through a tall pipe. The subsequently developed high-pressure devices were mainly of the piston-and-cylinder type.

At the beginning of the 19th century, pressures of about 400 MPa could be obtained, and at the beginning of the 20th century, often referred to as the end of the pre-Bridgman era, pressures up to about 2 GPa could be achieved. Then Percy W. Bridgman's remarkable inventions extended the pressure range greatly, to over 10 GPa (Bridgman, 1964). He devised new techniques for sealing pressure chambers, developed the opposed-anvils apparatus and introduced methods for the controlled measurement of various phenomena. Moreover, he used his new methods to describe a vast number of observations and properties of matter at high-pressure ranges hitherto unexplored. Bridgman's ingenious designs of high-pressure devices, such as the opposed-anvils apparatus, paved the path for future researchers. His scientific achievements won him the Nobel Prize in Physics in 1946.

The Bridgman era in high-pressure research ended in the late 1950s, when the diamond-anvil cell, often abbreviated to DAC, was invented (Weir *et al.*, 1959; Jamieson *et al.*, 1959; Piermarini, 2001). Soon after, the DAC became the main tool of high-pressure researchers; it gradually increased the range of attainable pressure by more than an order of magnitude, and under laboratory conditions it surpassed the pressure level at the centre of the Earth. Most importantly, the DAC allowed many new measuring techniques, particularly X-ray diffraction and optical spectroscopy, to be utilized. Before that, spectroscopic studies were limited to about 0.5 GPa. High-pressure X-ray diffraction, pioneered by Cohen (1933) in Berkeley for powders and by Vereshchagin *et al.* (1958) in Moscow for a single crystal of halite at 0.4 GPa in a beryllium high-pressure vessel, had been expensive, inefficient and inaccurate.

The DAC has become commonly available because of its low cost and easy operation. Today, the DAC continues to be the main and most versatile piece of laboratory pressure equipment and a record-breaking high-pressure apparatus. However, other sample environments provide complementary means of structural studies. For example, the large-volume press can be advantageous for neutron diffraction studies and in experiments where very stable high-pressure/high-temperature conditions are required. Naturally, the success of many high-pressure methods would not be possible without the development of other sciences and technologies, including computers, powerful sources of X-rays and neutrons and their detectors, and lasers.

2.7.3. Main types of high-pressure environments

High-pressure methods can be classified as dynamic or static. In the traditional dynamic methods, the pressure is generated for microseconds, usually at an explosion epicentre or at targets where ultra-fast bullets or gas guns are fired at the sample. The explosions are carried out either in special chambers or in bores underground (Batsanov, 2004; Ahrens, 1980, 1987; Keller *et al.*, 2012).

Even shorter, of a few nanoseconds' duration, the shock compression generated in targets using laser drivers coupled to the powerful X-ray pulses of a free-electron laser, or an otherwise generated X-ray beam, can further extend the attainable pressure limits. While this laser shock generates both high pressure and high temperature in the sample (the so-called Hugoniot compression path), in the ramp compression, also termed the off-Hugoniot path, the signal of the designed profile from an optical laser affords terapascal compression and approximates isothermal conditions (Wicks *et al.*, 2018; Smith *et al.*, 2014; Wang *et al.*, 2016).

The advantage of the gas and laser shock-wave and ramp-compression methods is that the attainable pressure is not limited by the tensile strength of the pressure chamber. Disadvantages include the inhomogeneous pressure, difficulties in controlling the temperature, the requirement for very fast analytical methods and the very high cost. The kinetic products generated during the explosion and in the shock waves can be different from the products recovered after the explosion, and different again from those formed under stable conditions. In most cases the laser-generated shock annihilates the sample.

Static methods are at present more suitable for crystallographic studies. The first variable-temperature sample-environment devices for structural studies of liquids and solids were designed soon after the inception of X-ray diffraction analysis. Structural investigations at high and low temperature at ambient pressure were mainly performed either by blowing a stream of heated or cooled gas onto a small sample (Abrahams *et al.*, 1950) or by placing the sample inside an oven or a cryostat. At present, a variety of attachments for temperature control are commercially available as standard equipment for X-ray and neutron diffractometers. Open-flow coolers using gaseous nitrogen and helium are capable of maintaining temperatures of about 90 K and a few kelvin, respectively, for days and weeks. They are easy to operate and pose no difficulties for centring the sample crystal, because the crystal is mounted, as in routine experiments, on a goniometer head with adjustable x–y–z translations and is visible at all positions through a microscope attached to the diffractometer. Cryostats and furnaces obscure the visibility of the sample and are usually heavy, and hence require strong goniometers; however, they often have the advantage of higher stability, a larger homogeneous area in the sample and a larger range of temperature (see Chapter 2.6).

Devices for static high-pressure generation are more difficult to construct because of the obvious requirement for strong walls capable of withstanding the high pressure applied to the sample. There are several types of high-pressure device and they can be classified in several ways. The piston-and-cylinder (PaC) press is the oldest type of pressure generator. However, the pressure range is limited in most advanced constructions (of multilayer negatively strained cylinders, like one shown in Fig. 2.7.1) to 3.0 GPa (Baranowski & Bujnowski, 1970; Besson, 1997; Dziubek & Katrusiak, 2014). PaC presses are ideal for volumetric measurements on a sample enclosed in the cylinder and for generating pressure in a hydrostatic medium transmitted through a capillary to other external high-pressure chambers containing the sample and optimized for a chosen measurement method, usually optical spectroscopy and diffraction. The external devices include chambers for loading the PaC with gas, which is either the hydrostatic medium or the sample itself (Tkacz, 1995; Rivers *et al.*, 2008; Couzinet *et al.*, 2003; Mills *et al.*, 1980; Yagi *et al.*, 1996; Kenichi *et al.*, 2001). In some pressure generators, a cascade of two or three PaC presses is applied for highly compressible pressure-transmitting media (gases) before the final setup stage.

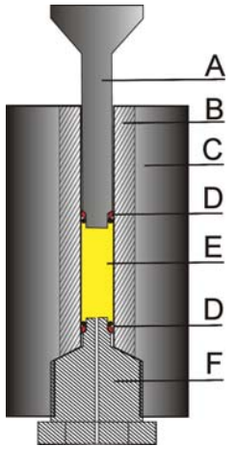

Figure 2.7.1
A cross section through a piston-and-cylinder device with a shrink-fitted double cylinder. In this design, the bottom piston (stopper F) is in the fixed position and only the top piston (A) is pushed into the cylinder by a hydraulic press. The main components of the device are: piston (A), inner cylinder (B), outer supporting shell (C), brass and rubber sealing rings (D), sample (E) and stopper (F).

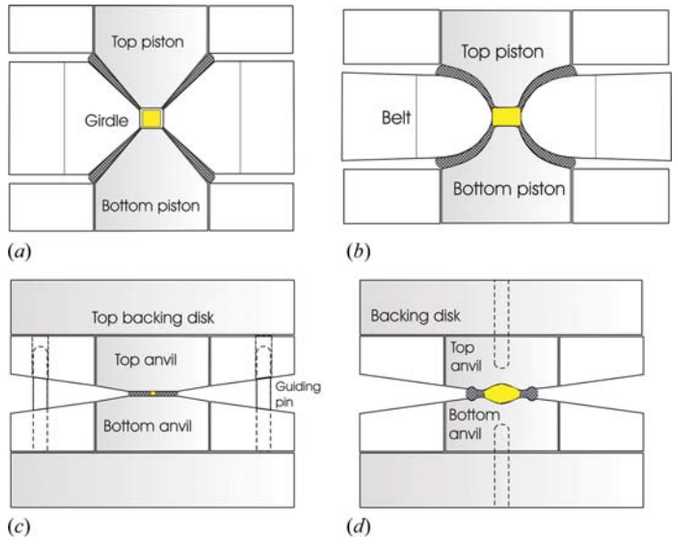

Figure 2.7.2
Cross sections of (*a*) the girdle anvil, (*b*) the belt anvil, (*c*) the Bridgman anvil and (*d*) the toroid anvil. The gaskets are dark grey, the tungsten carbide elements are pale grey and the sample chamber is yellow.

The PaC press can be considered as the prototype of other large-volume presses (LVPs). The PaC press consists of a cylinder closed at both ends with pistons, sealed with gaskets. The attainable pressure depends mainly on the tensile strength of the cylinder and of the gasket. The cylinder can be strengthened by the process of frettage, *i.e.* inducing tensile strain in the outer part and compressive strain inside (Onodera & Amita, 1991). This can be achieved by autofrettage, when a one-block cylinder is purposely overstrained to the point of plastic deformation and the deformation residues result in the required strain. Likewise, the cylinder can be built of shrink-fitted inner and outer tubes (the outer diameter of the inner tube is slightly larger than the inner diameter of the outer tube, which must be heated to assemble the cylinder) or of cone-shaped tubes (with a cone half-angle of *ca* 1°) pushed into one another to generate the frettaging strains. Alternatively, a coil of several layers of strained wire or tape can be wound around the cylinder, or the cylinder can be compressed externally to counteract its tensile strain simultaneously with the load being applied to the pistons (Baranowski & Bujnowski, 1970). The load against the cylinder walls can be reduced by containing the sample in a capsule of soft incompressible material, usually lead (Bridgman, 1964). Cylinder chambers with externally generated pressures up to 0.4 GPa (Blaschko & Ernst, 1974) and PaC cells capable of generating 2 GPa (Bloch *et al.*, 1976; McWhan *et al.*, 1974) have been used for neutron diffraction, and a beryllium cylinder has been used for X-ray diffraction on protein crystals to 100 MPa (Kundrot & Richards, 1986). The range of pressure up to a few hundred megapascals is often described as medium pressure. There are sample-environment chambers with externally generated medium pressure that are designed for in-house powder diffractometers operating in the Bragg–Brentano geometry (Koster van Groos *et al.*, 2003; Whitfield *et al.*, 2008).

If the cylinder length is reduced and the gasket reinforced by compression of the conical pistons, the girdle press is obtained (Fig. 2.7.2*a*). Its optimized modification is the belt apparatus (Fig. 2.7.2*b*). The girdle and belt presses generate pressures of about 10 GPa and can be internally heated to about 1500 K, and hence they have been used widely to synthesise materials. However, the opacity of the girdle/belt and anvils allows no access for X-ray or neutron beams between the anvils. This disadvantage is alleviated in the opposed-anvils press, operating on the massive-support principle, where the beams can pass through the gasket material. After the first record of a simple version of the opposed-anvils experiment in the mid 19th century performed in order to measure the effect of medium pressure on the electric conductibility of wires by Wartmann (1859), the opposed anvils were extensively developed and applied to much higher pressure by Bridgman (1935, 1941, 1952). He also equipped them with a pyrophyllite gasket separating the anvil faces (Bridgman, 1935), and in this form they are commonly known as Bridgman anvils (Fig. 2.7.2*c*). In the 1960s, the flat faces of the Bridgman anvils were modified to so-called toroidal anvils (Fig. 2.7.2*d*), where the sample space is considerably increased by hemispherical depressions at the anvil centre and surrounded by a groove supporting the gasket and preventing its extrusion (Khvostantsev, 1984; Khvostantsev *et al.*, 1977, 2004; Ivanov *et al.*, 1995). Anvils with a spherical sample cavity only, so-called Chechevitsa anvils, preceded the construction of toroidal anvils. Toroidal anvils were optimized for neutron diffraction by adding a small pneumatic press called the Paris–Edinburgh cell (Besson *et al.*, 1992). Toroidal anvils enabled neutron diffraction studies up to 50 GPa and 3000 K (Kunz, 2001; Zhao *et al.*, 1999, 2000; Redfern, 2002). Experiments on magnetic systems in a similar pressure range and at low temperature were performed in a very different design of opposed anvils, the sapphire Kurchatov–LBB cell, shown in Fig. 2.7.3 (Goncharenko & Mirebeau, 1998; Goncharenko, 2004).

More complex LVPs have been based on multi-anvil presses (Liebermann, 2011). These are usually very large devices capable of containing tens of cubic centimetres of sample. The sample is encapsulated and pressurized between anvils sealed with some kind of gasket. The attainable pressure depends on a number of factors, including the applied load and the strength of the anvils, which are made of steel, tungsten carbide, sapphire or sintered diamond; the maximum pressure depends inversely on the sample volume. Multi-anvil presses (Huppertz, 2004; Liebermann, 2011) – tetrahedral, trigonal–bipyramidal, cubic (Akimoto *et al.*, 1987) and octahedral (Onodera, 1987) – are optimized for larger sample volumes and for the high temperatures required for the synthesis of hard materials, especially diamond (Hazen, 1999). The multi-anvil presses are used for diffraction studies.

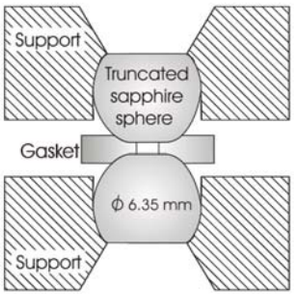

Figure 2.7.3
A schematic view of the opposed-sapphire anvil of the Kurchatov–LBB cell designed for neutron diffraction on magnetic materials (Goncharenko, 2004).

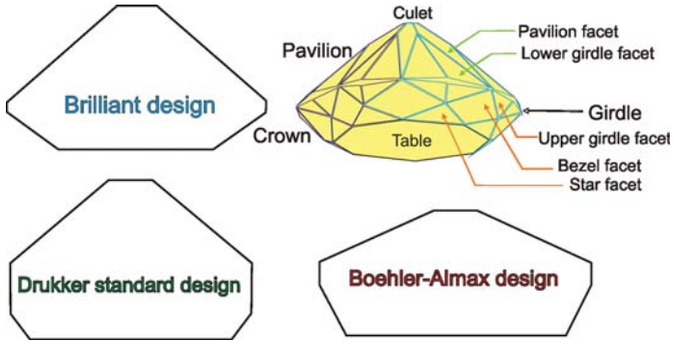

Figure 2.7.4
Cross sections of three types of diamond anvil used in high-pressure cells: the brilliant design (supported either on the table or on the crown rim), the Drukker design (supported on the table and crown) and the Boehler–Almax design (supported on the crown).

The sample can be either contained in a capsule or mixed with a pressure-transmitting pseudo-hydrostatic medium, which is inert and a weak absorber of X-rays. The sample is accessed by the X-ray beam between the anvils through a weakly absorbing sealing material, such as amorphous boron, magnesium oxide, corundum or pyrophyllite. Like the opposed-anvil presses, multi-anvil LVPs can be used effectively for X-ray diffraction at synchrotrons and neutron sources. However, these large installations also require (apart from intense primary beams) powerful translations for their precise centring relative to the primary beam and diffractometer axes. The main advantage of an LVP is stable and homogenous internal heating up to about 2000 K (Besson, 1997). Such stable conditions are particularly valuable for high-pressure synthesis and crystallization, for example of diamonds (Hazen, 1999).

2.7.4. The diamond-anvil cell (DAC)

The invention of the DAC revolutionized high-pressure studies, diversified their scope, greatly simplified the experimental procedures, increased the range of pressure and temperature, and initiated constant growth in the number of high-pressure structural studies, starting in the 1960s and continuing up to today. The DAC is built from a pair of opposing diamond anvils and a vice to generate their thrust. The sample is compressed between the culets of the anvils. Since its inception, the DAC has been modified and redesigned frequently, in order to adapt it to new experimental techniques or to take advantage of the parallel progress in scientific equipment. The original DAC built at the National Bureau of Standards (Maryland, USA) was used for infrared spectroscopy. Another DAC designed for powder diffraction experiments was made of beryllium, a relatively strong metal which weakly absorbs short-wavelength X-rays (Weir *et al.*, 1959; Bassett, 2009). The DAC, with steel frames and beryllium discs supporting the anvils, is still in use today.

The original and most efficient concept applied in the operation of the DAC was that the incident beam enters the pressure chamber through one diamond anvil and the reflections leave through the other anvil; this mode of operation is often referred to as transmission geometry. Together with the diamond anvils, Be discs constitute windows for the X-rays. However, beryllium has several disadvantages. It is the softest and weakest of the materials used in DAC construction, it softens at about 470 K, beryllium oxide is poisonous, and machining beryllium is difficult and expensive. Therefore, except for the pioneering DAC design by Weir *et al.* (1959), Be parts were initially limited to disc supports for the anvils. Moreover, polycrystalline Be discs produce broad reflection rings and a strong background, and the small central hole in the disc obscured optical observation of the sample. In many modern DACs the beryllium discs have been completely eliminated, and the diamond anvils are directly supported by steel or tungsten carbide platelets (Konno *et al.*, 1989; Ahsbahs, 2004; Boehler & De Hantsetters, 2004; Katrusiak, 2008). For this purpose new diamond anvils, exemplified in Fig. 2.7.4, were designed. Anvils of different sizes, culet dimensions, height-to-diameter ratios and other dimensions can be adjusted for the experimental requirements, such as the planned pressure range and the opening angles of the access windows.

Another DAC was independently designed for X-ray powder diffraction by Jamieson *et al.* (1959). In their DAC, the incident beam was perpendicular to the axis through the opposed anvils, and the primary beam passed along the sample contained and squeezed directly (no gasket was used) between the culets. The reflections were recorded on photographic film located on the other side of the DAC, perpendicular to the incident beam. This geometry was described as either panoramic, perpendicular or transverse. The transverse geometry is also used with beryllium or other weakly absorbing gaskets (Mao *et al.*, 1998). Other DACs, for example where both the incident beam and the reflections pass through one diamond anvil, were also designed (Denner *et al.*, 1978; Malinowski, 1987); however, the transmission geometry is most common owing to its advantages. In the transmission geometry the uniaxial support of the anvils leaves a window for optical observation of the sample, as well as for spectroscopic and diffractometric experiments along the cylindrical pressure chamber. Therefore, at present most DAC designs operate in transmission geometry.

The DAC construction can generally be described as a small vice generating thrust between opposed anvils. In the first DACs designed in the late 1950s, no gasket nor hydrostatic fluids were used and the sample was exposed to strong anisotropic stresses. Van Valkenburg (1962) enclosed the sample in a hole in a metal gasket, filled the hole with hydrostatic fluid and sealed it between the culets of the anvils. This most significant development of the miniature high-pressure chamber opened new possibilities for all sorts of studies under hydrostatic conditions, in particular powder and single-crystal diffraction studies. Since then, the gaskets have become an intrinsic part of the DAC. The hydrostatic conditions in the DAC have been used to grow *in situ* single crystals from the melts of neat compounds (Fourme, 1968; Piermarini *et al.*, 1969) and from solutions (Van Valkenburg *et al.*, 1971*a*,*b*). Now it is a common method for *in situ* crystallization under isothermal and isochoric conditions (Dziubek & Katrusiak, 2004; Bujak *et al.*,

2004; Fabbiani *et al.*, 2004; Fabbiani & Pulham, 2006; Budzianowski & Katrusiak, 2006*a*,*b*; Dziubek *et al.*, 2007; Paliwoda *et al.*, 2012; Sikora & Katrusiak, 2013).

The original designs of the DAC (Weir *et al.*, 1959; Jamieson *et al.*, 1959) were later adapted to various purposes. Significant modifications take advantage of new designs of diamond anvils and their supports. Initially, the brilliant-cut diamonds of traditional design, but with the culet ground off to form a flat thrust surface parallel to the table, were used (Fig. 2.7.4). Culets of 0.8 mm in size can be used to about 10 GPa, 0.4 mm culets to about 50 GPa, 0.1 mm culets to about 100 GPa and 0.02 mm (20 µm in diameter) or even smaller (Akahama *et al.*, 2014; Akahama & Kawamura, 2010; Dalladay-Simpson *et al.*, 2016) culets can be used for the megabar 200–400 GPa range. The megabar range requires bevels on the culets to protect their edges from very high strain and damage. The bevels are about 6–7° off the culet plane and the ratio of bevel-to-culet diameters is between 10 and 20. Also, the gasket material, the hole diameter and its height, being a fraction of the hole diameter, are of primary importance. Double bevels can be used to release the strain further, but it appears that a value of about 400 GPa is the maximum pressure attainable in the conventional DAC (c-DAC).

The pressure limits of the c-DAC are surpassed in a double-stage DAC (ds-DAC), in a toroidal DAC (t-DAC) or by shock compression. In the ds-DAC a pair of small anvils, constituting a microscopic DAC (m-DAC, also described as second-stage anvils), is contained inside the c-DAC. The micro-anvils are prepared from diamond or amorphous diamond using the focused ion-beam technique (Sakai *et al.*, 2015, 2018). For another type of ds-DAC, employing microscopic diamond hemispheres (Dubrovinsky *et al.*, 2012; Dubrovinskaia *et al.*, 2016), pressures exceeding 1 TPa have been reported. In the t-DAC, each diamond culet is modified in such a way that an ion-beam-eroded groove surrounds the central micro culet (Dewaele *et al.*, 2018; Jenei *et al.*, 2018; Mao *et al.*, 2018).

At present, the DAC most commonly applied in laboratories is a miniature Merrill–Bassett DAC, where the anvils are installed on two triangular frames driven by three screws along three sliding pins (Merrill & Bassett, 1974). Analogous designs with two or four thrust-generating screws are also in use. The original Merrill–Bassett DAC was equipped with a pair of brilliant-cut 0.2 carat diamonds with polished culets (Fig. 2.7.4) and the anvils were supported on Be discs. The Merrill–Bassett DAC is optimized for use with automatic diffractometers. It contains no rocking blocks but allows translation of one of the anvils. The light weight and small size allow the Merrill–Bassett cell to be routinely used on single-crystal diffractometers. This simple DAC design is suitable for experiments up to about 10 GPa. Dedicated DACs for higher pressure have rocking supports for the diamonds, in the form of either hemispheres or half-cylinders (Fig. 2.7.5).

A very fine adjustment of the anvils and fine and remote pressure control can be obtained in a membrane DAC, where the thrust is generated by a metal membrane operated with gaseous helium or nitrogen (Letoullec *et al.*, 1988; Chervin *et al.*, 1995). Owing to the ideally coaxial thrust generation by the membrane and the stable supports of the anvils, usually in the form of a piston and cylinder, the membrane DAC is suitable for generating pressures of hundreds of gigapascals. The membrane DAC can be operated remotely through a flexible metal capillary, which is advantageous for spectroscopy and both powder and single-crystal diffraction experiments at synchrotrons.

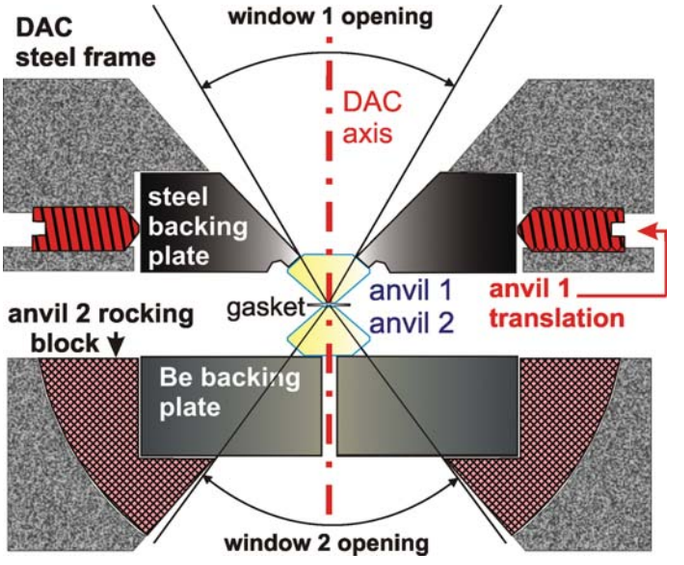

Figure 2.7.5
A cross section through the central part of a diamond-anvil cell, schematically showing the main elements applied in various designs. Usually, either beryllium backing plates or steel/tungsten carbide backing plates with conical windows are used. One of the plates can be translated and the other rocked in all directions (the hemispherical rocking mechanism). In other designs, one of the anvils can be rocked around and translated along one axis, and the other anvil rocked and translated in the perpendicular direction (two perpendicular hemicylindrical mechanisms). The usual thickness of the beryllium plate is 3 mm or more, and most constructions allow a window opening of about 40° to the DAC axis. The thickness of the diamond window (the table-to-culet distance) is usually about 1.5 mm.

2.7.5. Variable-temperature high-pressure devices

One of the most common interests in extreme conditions combines high pressure and high temperature. Several techniques for simultaneously controlling both pressure and temperature have been developed (Fei & Wang, 2000). The DAC can be heated externally (with respect to the sample chamber between the anvils' culets) when the entire DAC is placed in an oven or in a hot stream of air from an electrical heater (Fourme, 1968; Allan & Clark, 1999; Podsiadło & Katrusiak, 2008; Bujak *et al.*, 2008). External resistance-wire heaters placed immediately around the diamond anvils and the gasket are often used (Bassett & Takahashi, 1965; Takahashi *et al.*, 1982; Adams & Christy, 1992; Eremets, 1996; Moore *et al.*, 1970; Hazen & Finger, 1982; Besson, 1997; Dubrovinskaia & Dubrovinsky, 2003; Fei & Wang, 2000). External heating can routinely operate up to about 673 K. Its main advantages are stability, reliable measurement of temperature and high homogeneity of temperature in the chamber. The disadvantages include the relatively low temperature range and the large mass of the DAC mechanical parts that are heated. Their thermal expansion can cause loss of pressure. This does not apply to the membrane DAC, where a constant thrust from the membrane is transmitted to the anvils. A sophisticated externally heated DAC in an atmosphere of inert gases is capable of operating between 83 and 1473 K (Bassett *et al.*, 1993).

A very small turnbuckle DAC, about 6 mm in diameter, was originally constructed of plastic and hardened beryllium–copper alloy (BERYLCO 25) in order to perform magnetic measurements at low temperature in the small bore of a superconductive quantum interference device (SQUID) (Graf *et al.*, 2011; Giriat *et al.*, 2010). These are at present the smallest designs that can be

used for X-ray diffraction studies, with the whole DAC cooled by commercial low-temperature gas-stream attachments. Alireza & Lonzarich (2009) built another miniature DAC for high-pressure magnetic measurements in a SQUID.

Temperatures of several thousand kelvin can be achieved by internal heating, where the sample absorbs the focused light beam of a laser (Bassett, 2001; Ming & Bassett, 1974; Shen *et al.*, 1996) or is heated by a thin wire passing through the chamber or its immediate surroundings, either in the gasket walls (Boehler *et al.*, 1986; Mao *et al.*, 1987; Zha & Bassett, 2003; Dubrovinsky *et al.*, 1998) or in the culets of intelligent diamond anvils (Bureau *et al.*, 2006). Composite resistance gaskets, with a platinum chamber wall acting as a 35 W resistance heater, can increase the temperature to over 2273 K (Miletich *et al.*, 2000, 2009). Laser beam(s) focused through the DAC anvil(s) onto the sample (Boehler *et al.*, 2001) can heat it to over 3273 K. This requires that the laser beam, or several beams, or a fraction of their energy, be absorbed in the sample. In order to increase the absorption, the sample can be mixed with another compound, for example gold powder. The main disadvantage of laser heating is inhomogeneous distribution of the temperature within the sample.

Much smaller temperature gradients, of a few kelvin at 2773 K, can be obtained in large-volume presses (LVPs). The multi-anvil LVP has traditionally been applied for the synthesis of diamond, which requires stable conditions of both high pressure and high temperature (Hazen, 1999; Liebermann, 2011). In the LVP, a resistance heater installed inside the chamber can provide stable control of the temperature for days, while the pressure is controlled by a hydraulic press. Owing to the large sample volume, the diffraction pattern can be quickly recorded. Most often, energy-dispersive diffraction is applied for the beams entering and leaving the pressure chamber through the gasket material between the anvils. LVPs are generally very large and heavy, which contrasts with the compact construction of the Paris–Edinburgh and Kurchatov–LLB pressure cells (Besson *et al.*, 1992; Goncharenko, 2004, 2006). Both these opposed-anvil cells can be placed in cryostats, and they can be used for either energy- or angle-dispersive diffraction of neutrons or X-rays. The Kurchatov–LLB cell has been optimized for neutron diffraction studies of magnetic structures at high pressure and low temperature (Goncharenko & Mirebeau, 1998; Goncharenko *et al.*, 1995).

2.7.6. Soft and biomaterials under pressure

Interest in the effects of pressure on biological materials is connected to the processing of food and the search for methods of modifying the structure of living tissue and its functions. Soft biological compounds, including proteins, membranes, surfactants, lipids, polymer mesophases and other macromolecular assemblies present in living tissue, are susceptible to pressure, which can affect the molecular conformation and arrangement with relatively low energies of transformation (Royer, 2002). Medium pressure suffices for protein coagulation, as observed for egg white at 0.5 GPa by Bridgman (1914). However, single crystals of egg-white lysozyme survived a pressure of several gigapascals (Katrusiak & Dauter, 1996; Fourme *et al.*, 2004), which was connected to the concentration of the mother liquor used as the hydrostatic fluid. Cells with externally generated pressures up to about 200 MPa for diffraction measurements on single crystals in a beryllium capsule (Kundrot & Richards, 1986) and on powders contained between beryllium windows (So *et al.*, 1992) have been built. Powder diffraction studies have also been performed on samples frozen under high pressure and recovered to ambient pressure (Gruner, 2004). High-pressure studies can be conveniently performed in the DAC, but because of the usually weak scattering of macromolecular samples, synchrotron radiation is preferred for such experiments (Fourme *et al.*, 2004; Katrusiak & Dauter, 1996).

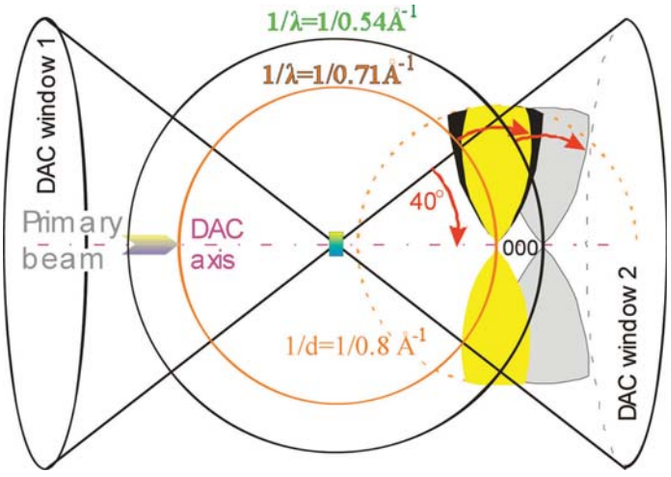

Figure 2.7.6
A diamond-anvil cell, showing the 40° half-angle opening of the conical windows and the reciprocal space accessed for a single-crystal sample and Mo $K\alpha$ or Ag $K\alpha$ radiation. In this schematic drawing, the window cones intersect at the disc-shaped sample (yellow–blue shaded rectangle) and around it the Ewald spheres of reciprocal radii corresponding to Mo $K\alpha$ and Ag $K\alpha$ wavelengths are drawn. The shape of the two yellow profiles meeting at the reciprocal 000 node is the cross section through the torus-like accessible volume of reciprocal space for Mo $K\alpha$ radiation; this torus is circularly symmetric about the DAC axis. The grey shape is likewise the accessible space for Ag $K\alpha$ radiation. Both are at the same resolution of $1/d_{hkl} = 1/0.8$ Å^{-1} (corresponding to θ angles of 26.4° for Mo $K\alpha$ radiation and 19.7° for Ag $K\alpha$). For a powdered sample, all reciprocal-space nodes contained within the resolution sphere (dotted circle) can be recorded. The DAC windows and the sample are shown at the initial 'zero' position, when the DAC axis coincides with the primary beam; the red arrows indicate the rotation of the DAC, sample and Ewald sphere to the limiting 40° angle.

2.7.7. Completeness of data

The steel parts of the DAC can restrict access of the incident beam to the sample and can obscure the exit of reflections. For a typical DAC working in transmission mode, the incident beam can be inclined to the DAC axis by up to about 25–40°, for the full opening of the window of 50–80°, respectively. In most DACs the collimator and detector sides are symmetric, so the opposing conical windows have the same opening angle. This limited access to the sample can affect the completeness of diffraction data for low-symmetry crystals, which can then pose considerable difficulties in solving and refining crystal structures from single-crystal measurements.

The restricted access of the primary and diffracted beams to the sample can conveniently be described by the concept of the reciprocal lattice (Fig. 2.7.6). The initial orientation of the crystal in the DAC defines the accessible region of the reciprocal lattice in such a way that the Ewald sphere can be inclined to the initial direction of the incident beam by up to the maximum window opening angle, denoted α_M. The sample can be accessed from both sides of the DAC (by rotating the DAC by 180°) and thus the accessible region of reciprocal space has the form of a round flat cushion, with surfaces touching at the cushion centre [described

as a donut cake by Merrill & Bassett (1974)], as shown in Fig. 2.7.6. In the directions perpendicular to the DAC axis, the maximum coordinate $d^*_{yz} = 2\lambda^{-1} \sin \alpha_M$ of reciprocal vectors is for many crystals larger than the resolution of the data (for a typical DAC, $\alpha_M = 40^\circ$, which for organic crystals or other weakly scattering substances is less than required, as the data measured with Mo $K\alpha$ radiation for molecular crystals often extend up to a maximum θ of only about 25°). However, access to the reciprocal lattice is significantly limited along the DAC axis (perpendicular to the flat cushion). In this direction, only those reflections can be accessed for which

$$d^*_x = 2\lambda^{-1} \sin^2(\alpha_M/2),$$

where d^*_x is the maximum coordinate of accessible reciprocal vectors along the x_L axis running from the sample to the radiation source in the laboratory reference system, λ is the wavelength, and α_M is the opening angle of the window measured from the DAC axis (or the maximum inclination of the DAC axis to the incident beam). For example, a DAC with a full window opening angle of $2\alpha_M = 60^\circ$ limits the laboratory reciprocal x coordinate to 0.1885 Å^{-1} when λ(Mo $K\alpha$) = 0.71073 Å is used; if the crystal x^* axis is aligned along the laboratory x_L axis, and if the crystal a^* = 0.10 Å^{-1}, then the maximum Bragg reflection index $|h|$ is 1. If the wavelength is decreased to λ(Ag $K\alpha$) = 0.56 Å, the maximum d_x increases to 0.2392 Å^{-1} and reflections with index h = 2 can be recorded.

Although the accessible region of the reciprocal lattice depends strongly on the DAC design, the final completeness of the data also depends on several other factors: (i) the symmetry of the sample crystal; (ii) the sample orientation; and (iii) the wavelength of the X-ray radiation. Therefore, the DAC is ideally suited to high-pressure studies of simple and high-symmetry crystals. The Laue-class symmetry of cubic crystals is either $m\bar{3}$ or $m\bar{3}m$, and in most cases the whole of the required resolution falls within the accessible flat-cushion reciprocal region. Thus, the completeness in high-pressure experiments on cubic samples mounted in the chamber at a random orientation is not limited. For hexagonal and tetragonal samples, the crystal orientation is very significant. The maximum completeness can be obtained when the hexagonal or tetragonal axis is perpendicular to the DAC axis. Then the sample reciprocal axis c^* is located along the flat-cushion plane. When two axes of a monoclinic or orthorhombic crystal are at 90° to the DAC axis, a considerable portion of the symmetry-independent part of the reciprocal lattice is not accessible. This reduces the completeness of the data, even though the redundancy of the data is increased. Optimum orientation of the sample can double the completeness compared with experiments measured for the same sample with its axes aligned along the DAC axis and plane.

The completeness of the data can be increased by collecting several data sets for samples oriented differently in the DAC and merging these data (Patyk *et al.*, 2012). This purpose can also be achieved by placing several crystal grains at different orientations in the high-pressure chamber, and then separating their reflections, indexing them and merging.

When the powder diffraction method is used, this problem of completeness is irrelevant. As shown in Fig. 2.7.7, for an ideal powder with randomly oriented grains all reciprocal-lattice nodes can be represented as spheres and they all satisfy the Bragg diffraction condition. The main problem occurring for samples with low symmetry and long lattice constants is overlapping reflections. The intensity of the powder reflection rings is low,

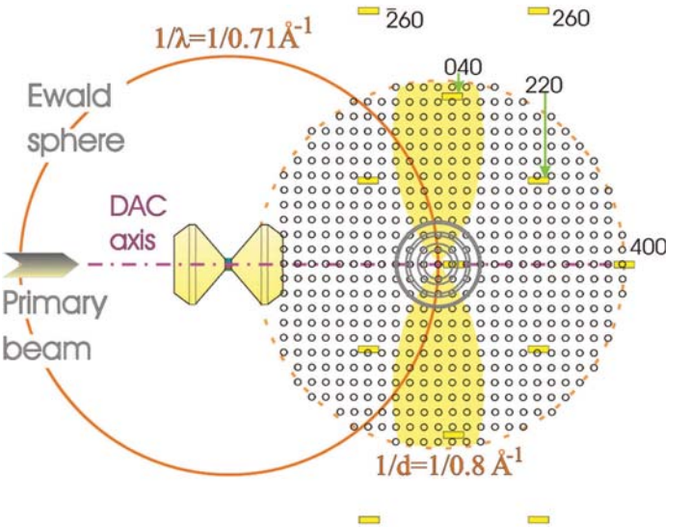

Figure 2.7.7
A schematic illustration of the reciprocal space associated with a sample enclosed in a diamond-anvil cell (DAC). For clarity, the sizes of the sample and diamond anvils have been increased. The Ewald sphere is drawn for the sample only and cubic symmetry with an a parameter of 10 Å has been assumed. Of the reciprocal lattice of the sample, only the layer of $hk0$ nodes is shown as small circles within the resolution limit of $1/d_{hkl}$ = 1/0.8 Å^{-1}. The Ewald spheres of the diamond anvils have been omitted, and only the layer of nodes $hk0$ of the detector anvil is shown as yellow rectangles. Owing to its short unit-cell parameter of 3.57 Å and $Fd\bar{3}m$ symmetry, there are few diamond reflections in the pattern. Note the displaced origins of the reciprocal lattices of the sample and of the detector anvil (the anvil on the detector side) as a result of the off-centre positions of the anvil. For a powdered sample, each node is distributed on a sphere. In this drawing, the spheres are represented by circles only for nodes 100, 110, 200, 210, 220 and 300. The other node spheres contained within the chosen resolution limit have been omitted for clarity; for a triclinic sample, the $hk0$ layer would include 266 powder reflections.

because only a small fraction of the sample volume, less than one part per million, contributes to the intensity at a specific point on the reflection ring. Furthermore, the sample volume in the DAC is very small. For these reasons, powder X-ray diffraction in the laboratory usually provides only qualitative information. After the introduction of synchrotron radiation and area detectors, powder diffraction became one of most efficient methods of high-pressure structural studies.

2.7.8. Single-crystal data collection

It is essential that a crystal sample is centred precisely on the diffractometer. Optical centring of a crystal is hampered by the limited view of the sample through the DAC windows in one direction only and by the strong refractive index of diamonds. Consequently, diffractometric methods of crystal centring are more precise for DAC centring. Hamilton's method comparing the diffractometer setting angles of reflections at equivalent positions (Hamilton, 1974) was modified for the purpose of the DAC by King & Finger (1979) and then generalized for any reflections, not necessarily at equivalent positions (Dera & Katrusiak, 1999). These methods are very precise, but they require the approximate orientation matrix (UB matrix) of the sample crystal (Busing & Levy, 1967) to be known and the reflections to be indexed. This information was determined at the beginning of an experiment when traditional diffractometers with a point detector were used. However, nowadays diffractometers with area detectors are used, and generally the crystal orientation

is not determined before collecting the diffraction data. To meet these requirements, a new efficient and semi-automatic method was devised, whereby the diffractometer measures a sequence of shadows of the gasket on the CCD detector and calculates the required corrections to the DAC position along the goniometer-head translations (Budzianowski & Katrusiak, 2004). Precise centring can only be achieved for very stable goniometer heads that do not yield under the weight of the DAC (Katrusiak, 1999).

The mode of data collection for a sample enclosed in a DAC can affect the data quality considerably. Data for a bare crystal on a four-circle diffractometer with a scintillation point detector were measured in the so-called bisecting mode, where the ω angle [diffractometer-axes positioning angles ω, χ, φ and θ of the Eulerian cradle will be used here (Busing & Levy, 1967), unless otherwise noted] was fixed to 0° and not used in the process of crystal positioning. In other words, the shaft φ and circle χ lie in the plane bisecting the angle formed by the incident beam and the reflection actually measured. The bisecting mode was optimal for avoiding collisions between the diffractometer shafts and detector, and also minimized absorption effects for most vertically mounted samples. However, these features are irrelevant for samples enclosed in a DAC. It was shown by Finger & King (1978) that the DAC absorption of the incident and reflected beams is a minimum when the Eulerian goniometer φ axis is not used and is always set to 0°. Hence, this is called the $\varphi = 0°$ mode. The $\varphi = 0°$ mode also minimizes the effect of the sample being shadowed by the gasket edges (Katrusiak, 2008). Moreover, in the $\varphi = 0°$ mode the DAC axis always lies in the diffraction plane of the diffractometer, which gives maximum access to the reciprocal-lattice nodes (Fig. 2.7.6).

The advent of area detectors facilitated high-pressure experiments considerably and extended the range of attainable conditions to simultaneous very high pressure and temperatures of several thousand kelvin. Single-crystal experiments are easier because the diffraction data can be recorded before the orientation matrix UB of the crystal is determined (Busing & Levy, 1967; Finger & King, 1978). The recorded data can thus be analysed after the experiment and all relevant structural models can be tested. The use of area detectors shortens the data-collection times for both single-crystal and powder diffraction measurements, and this is particularly efficient with the extremely intense X-ray beams provided by synchrotrons. In single-crystal experiments, several or even tens of reflections are partly scanned through or fully recorded in one image. Although these reflections are not each recorded at their optimum diffractometer settings, corresponding to the $\varphi = 0°$ mode setting described above, the redundancy of the data is increased and the intensities can be corrected for the absorption coefficients derived from differences between equivalent reflections. It is also advantageous that simultaneous diffraction events in the sample crystal and in one or both of the diamonds, which occur sporadically and weaken the recorded reflections, can be eliminated by comparing the intensities of the same reflection measured at several ψ angle positions as well as the equivalent reflections. Equivalent reflections measured at different positions are particularly useful for eliminating systematic errors in the data collection.

It is important that the so called 'run list', defining the diffractometer setting angles and scan directions for the detector exposures, takes into account the $\varphi = 0°$ mode of the DAC orientations, for which access to the DAC is still on average at its widest and the DAC absorption and gasket-shadowing effects are on average the smallest. Most importantly, such an optimum setting can be executed with a four-circle diffractometer, and cannot be done on simplified diffractometers with the φ shaft fixed at a χ angle of about 50°. Even fewer reflections can be accessed when the DAC is rotated about one axis only, which is still the case for some laboratory and synchrotron diffractometers.

2.7.9. Powder diffraction with the DAC

The DAC is often described as the workhorse of high-pressure research, owing to its versatile applications, low cost, easy operation and unrivalled attainable static pressure. However, the small size of the DAC chamber, containing sample volumes between 0.025 mm^3 for pressure to about 5 GPa, 0.005 mm^3 to about 10 GPa and less than 3×10^{-6} mm^3 for the megabar range, can be disadvantageous for powder diffraction studies. The disadvantages include the inhomogeneous distribution of temperature within the sample (particularly as it remains in contact with a diamond, which is the best known thermal conductor) and nonhydrostatic strain (often due to the technique of generating pressure by uniaxial compression of the chamber). In some samples close to the melting curve some grains increase in size at the expense of others, partly or fully dissolving, so the number of grains may be insufficient for obtaining good-quality powder diffraction patterns. This difficulty can be partly circumvented by rocking the DAC during the experiment about the ω axis. On the other hand, for a sample consisting of tens of grains it is possible to perform multi-grain analysis by merging the diffraction patterns to give the equivalent of single-crystal data. High-pressure powder diffraction patterns can also be affected by a low signal-to-noise ratio, too few crystal grains, and their preferential orientation in the DAC uniaxially compressed chamber. The preferential orientation is particularly significant when the grains are elongated and their compressibility is anisotropic; these effects can be further aggravated by the non-hydrostatic environment. Powder reflections are much weaker in intensity than the equivalent single-crystal reflections from the same sample volume. Small sample volumes are compensated for by the powerful beams available at synchrotrons. At present, high-pressure powder diffraction experiments are mainly carried out at synchrotrons by energy-dispersive (Buras *et al.*, 1997*a*,*b*; Baublitz *et al.*, 1981; Brister *et al.*, 1986; Xia *et al.*, 1990; Oehzelt *et al.*, 2002) and angle-dispersive methods (Jephcoat *et al.*, 1992; Nelmes & McMahon, 1994; Fiquet & Andrault, 1999; Crichton & Mezouar, 2005; Mezouar *et al.*, 2005; Hammersley *et al.*, 1996). Angle-dispersive methods are currently preferred to the energy-dispersive method owing to their higher resolution and simpler data processing. However, the energy-dispersive method requires less access for the X-ray beams probing the sample, and hence it is often preferred for studies in the megabar range (hundreds of gigapascals). For high-pressure powder diffraction studies in the laboratory, energy-dispersive methods are still preferred (Tkacz, 1998; Palasyuk & Tkacz, 2007; Palasyuk *et al.*, 2004). The main advantages of experiments at synchrotrons are:

(i) They have a very intense beam compared with traditional sealed X-ray tubes and modern micro-focus sources;
(ii) They offer the possibility of very narrow collimation of the beam, to a diameter of one or a few micrometres;
(iii) Very quick collection of high-quality diffraction data is possible, which is most useful for high-pressure and very high temperature data collections;
(iv) It is possible to measure diffraction data from very small samples, to reduce the dimensions of the DAC chamber and

hence to increase the attainable pressure, which is inversely proportional to the chamber diameter;

(v) The microbeam can illuminate a small selected portion of the sample chosen for the investigation, which can be used to perform single-crystal diffraction on a selected grain or for X-ray tomography of the sample and its inclusions;

(vi) The beam diameter is smaller than the diameter of the chamber, which minimizes or even eliminates the effects of beam shadowing;

(vii) The X-ray wavelength is tuneable down to about 0.3 Å. This considerably increases the data completeness and reduces absorption effects in the sample and DAC.

Owing to these features, synchrotron beams are ideally suited for high-pressure diffraction experiments and some researchers have completely stopped using in-house laboratory equipment with sealed X-ray tubes. Historically, the first use of synchrotron radiation for high-pressure studies was reported by Buras, Olsen & Gerward (1977) and Buras, Olsen, Gerward *et al.* (1977). Conventional diffractometers with sealed X-ray tubes can be effectively used for preliminary powder diffraction experiments. For example, a new high-pressure phase of (+)-sucrose was found in this way (Patyk *et al.*, 2012), although the data were insufficient for any structural refinements.

Diffraction data are collected in single and multiple exposures, and the pressure is controlled remotely by inflating a membrane through a gas system. Currently assembled high-pressure powder diffraction synchrotron beamlines incorporate on-line pressure calibration using ruby fluorescence and, often, Raman spectroscopy.

2.7.10. Sample preparation

Several basic techniques can be used to prepare a sample for a high-pressure experiment, for example:

(i) A solid sample can be mounted under ambient conditions in the high-pressure chamber together with the hydrostatic fluid, then sealed and pressurized;

(ii) A solid sample can be mounted under ambient conditions in the high-pressure chamber, condensed gas loaded at elevated pressure (Tkacz, 1995; Rivers *et al.*, 2008; Couzinet *et al.*, 2003; Mills *et al.*, 1980; Yagi *et al.*, 1996; Kenichi *et al.*, 2001) or under cryogenic conditions, and the sample sealed and further pressurized by gasket compression;

(iii) A liquid sample can fill the whole chamber volume under ambient conditions, or condensed gases or their mixtures can be loaded at elevated pressure, and after sealing the DAC the sample is frozen under isothermal conditions;

(iv) A crystal of the pure compound or of a solvate can precipitate from the mixture (solution) when compressed isothermally – the crystal can be in the form of a single crystal or a powder, fully or partly filling the DAC chamber;

(v) Samples completely filling the DAC chamber can be compressed isothermally or undergo isochoric treatment, but strains can be generated in a single crystal or in the grains of a compressed powder conglomerate by anisotropic thermal contraction/expansion; this strain can be avoided by having an excess of the hydrostatic component of the mixture;

(vi) A solid powdered sample can be mixed with a powder of another compound, which is much softer than the sample and is used as a pseudo-hydrostatic medium (halite and MgO are often used for this purpose) – this technique is mainly used for cubic or isotropic samples in large-volume presses, where (pseudo)isotropic strain and pseudo-spherical compression minimize the effect of preferential orientation in the sample.

Preferential orientation can significantly hamper the quality of powder diffraction data, and corrections for this effect should be applied in the Rietveld refinement. All Rietveld refinement programs include preferential orientation models, which fit the data with satisfactory results (McMahon, 2004, 2005; Filinchuk, 2010).

2.7.11. Hydrostatic conditions

Hydrostatic conditions in the sample chamber are essential for good-quality high-pressure diffraction data. They are equally important for single-crystal and powder diffraction experiments. To secure hydrostaticity, the sample is submerged in a hydrostatic medium. The pressure and temperature ranges of the planned experiment depend on the hydrostatic properties of the applied medium. Eventually all substances solidify because of crystallization or vitrification (Piermarini *et al.*, 1973; Eggert *et al.*, 1992; Grocholski & Jeanloz, 2005), which can lead to damage of single crystals, anisotropic strain in powder grains and inhomogeneity of pressure across the sample. It is also important to protect a solid sample from dissolution in the hydrostatic fluid. The dissolved sample can lose its required features (such as shape, polymorphic form or chemical composition) and recrystallize at higher pressure in an undesired form. For example, a fine powder may recrystallize into a few large and preferentially oriented grains. Another potential problem can arise from reactions between the sample and the hydrostatic medium. For example, a pure compound can form solvates incorporating molecules of the hydrostatic fluid (Olejniczak & Katrusiak, 2010, 2011; Andrzejewski *et al.*, 2011; Tomkowiak *et al.*, 2013; Boldyreva *et al.*, 2002; Fabbiani & Pulham, 2006). This has also been observed for helium and argon penetrating into the structures of the fullerenes C_{60} and C_{70} (Samara *et al.*, 1993) and into arsenolite As_4O_6 (Guńka *et al.*, 2015). High-pressure crystallization of water in the presence of helium leads to an inclusion compound interpreted as ice XII. Therefore, the hydrostatic medium should be carefully chosen for a specific experiment, depending on the sample solubility, the pressure range and the type of investigation, whether a mounted-sample study, or *in situ* crystallization or reaction (Sobczak *et al.*, 2018; Półrolniczak *et al.*, 2018).

Many minerals and inorganic samples hardly dissolve at all and a commonly applied pressure-transmitting medium is a mixture of methanol, ethanol and water (16:3:1 by volume), hydrostatic to over 10 GPa at 296 K (see Table 2.7.1); separately, pure methanol crystallizes at 3.5 GPa, ethanol at 1.8 GPa and water at 1.0 GPa. If a sample dissolves well in methanol, ethanol and water, other fluids can be selected (Piermarini *et al.*, 1973; Angel *et al.*, 2007). Liquids like glycerine (hydrostatic to 3 GPa) and special inert fluids, such as silicone oil (Shen *et al.*, 2004; Ragan *et al.*, 1996), Daphne oil (Yokogawa *et al.*, 2007; Murata *et al.*, 2008; Klotz *et al.*, 2009), or condensed gases, like helium, argon and hydrogen (Tkacz, 1995; Dewaele & Loubeyre, 2007), can be used. Alternatively, a saturated solution of the sample compound, for example in a methanol–enthanol–water mixture, can prevent sample dissolution, but on increasing the pressure the compound can precipitate in the form of a powder or single crystals. One can choose to load an excess of the sample into the chamber before filling it up with the hydrostatic fluid, which would dissolve only some of the sample.

Table 2.7.1
The (pseudo)hydrostatic limits of selected media at 296 K (Holzapfel, 1997; Miletich *et al.*, 2000)

Medium	Freezing point (GPa)	(Pseudo)hydrostatic limit (GPa)	Reference
4:1 Methanol:ethanol	–	9.8	Angel *et al.* (2007)
16:3:1 Methanol:ethanol:water	–	10.5	Angel *et al.* (2007)
Anhydrous propan-2-ol	–	4.2	Angel *et al.* (2007)
Neon	4.7	19	Klotz *et al.* (2009)
Argon	1.2	9/35	Bell & Mao (1981)/You *et al.* (2009)
Helium	11.8	70/150	Bell & Mao (1981)/Dewaele & Loubeyre (2007)
Hydrogen	5.7	177	Mao & Bell (1979)
Nitrogen	2.4	13	LeSar *et al.* (1979)
Glycerol	–	1.4	Angel *et al.* (2007)
Glycerin	–	3.0	Hazen & Finger (1982)
Glycerin		4.0	Tateiwa & Haga (2010)
Fluorinert FC84/87	–	7.0	Klotz *et al.* (2009)
Petroleum ether	–	6.0	Mao & Bell (1979)
Isopropyl alcohol		4.3	Piermarini *et al.* (1973)
1:1 Pentane:isopentane	–	7.4	Piermarini *et al.* (1973)
Silicone oil, viscosity 0.65 cSt	–	0.9	Angel *et al.* (2007)
Silicone oil	–	14	Klotz *et al.* (2009)
Daphne oil 7373		2.3	Murata *et al.* (2008)
Daphne oil 7474		3.7 at 296 K/6.7 at 273 K	Klotz *et al.* (2009)/Tateiwa & Haga (2010)
Vaseline	–	2.0	Tateiwa & Haga (2010)
NaCl	–	0.05/25	Tateiwa & Haga (2010)/You *et al.* (2009)

In situ crystallization at high pressure requires good, though not necessarily very good, solvents. Also, co-crystallizations can be performed in the DAC, and in this case the product that is obtained can depend on the solvents used and their concentration. Pressure effectively modifies intermolecular interactions, and new solvates can be obtained depending on the concentration of the substrates. It can be tricky to avoid co-crystallization of some compounds; in these cases a range of hydrostatic fluids has to be tried. A mixture of petroleum ethers, silicone or Daphne oils can be a good choice. Daphne oil, consisting mainly of alkylsilane (Murata *et al.*, 2008), has the rare feature of negligible thermal expansion, which is particularly useful for low-temperature high-pressure experiments: the DAC can be loaded under normal conditions and then pressurized and cooled to the required temperature, *e.g.* in a cryostat, without significant loss of pressure due to contraction of the medium.

The hydrostatic conditions can be checked by inspecting the width of reflections from the sample (full width at half-maximum, FWHM, is usually plotted), the width of the ruby fluorescence R_1 line and the R_1–R_2 line separation (You *et al.*, 2009). The pressure homogeneity can be checked by measurements for several ruby chips mounted across the DAC chamber. Nonhydrostatic conditions can cause inconsistent results and difficulties in their interpretation, which can prompt the researcher to consider changing the hydrostatic medium.

For hard samples, some departure from hydrostatic conditions is often acceptable. It is assumed that for a hard sample the nonhydrostatic compression component is small in a much softer medium, for example, hard corundum studied in soft NaCl. On the other hand, it may be easier to prepare a sample under normal conditions by uniformly mixing the powder of the specimen with a pseudo-hydrostatic medium, rather than using hydrostatic liquids or gases. The diffraction from the pseudo-hydrostatic medium powder can be used to monitor the pressure and measure non-hydrostaticity effects. Pseudo-hydrostatic solid media are often used for multi-anvil presses, where a solid sample facilitates loading and the uniaxial stress is not as drastic as in the opposed-anvil presses. Also, in high-temperature experiments the process of annealing reduces non-hydrostatic strain.

A relatively low nonhydrostatic effect was reported for argon frozen at 1.9 GPa: its pressure gradient up to 1% only is supported at 9 GPa (Bell & Mao, 1981) and up to 1.5% at 80 GPa (Liu *et al.*, 1990). This illustrates how the pseudo-hydrostaticity limit can be extended depending on the hardness of the specimen, the type of high-pressure device and the acceptance of deviatoric stress in the sample.

At very high pressure, exceeding 60 GPa, no compounds persisting as liquids are known (*cf.* Table 2.7.1). Diffraction data must then be corrected for a deviatoric stress component, causing the broadening of reflection rings and affecting their $2\theta_{\rm Bragg}$ positions, when the uniaxial stress is not collinear with the incident beam (Singh, 1993; Singh & Balasingh, 1994; Singh *et al.*, 1998; Mao *et al.*, 1998). The effect of uniaxial stress can be reduced or eliminated by sample annealing, which is often applied to improve the hydrostaticity of the sample.

2.7.12. High-pressure chamber and gasket in the DAC

A high-pressure device should be adjusted to the experiments planned, and in particular to the chemical activity of the sample. Gaseous hydrogen penetrates and dissolves in most metals, and therefore special alloys, such as beryllium bronze, have to be used for hydrogen setups. For some experiments non-metallic gaskets can be used, for example amorphous boron, corundum or diamond powders mixed with a resin. Owing to the insulating properties of such a gasket, the pressure dependence of the electric, dielectric and magnetic properties of the sample can be measured. Chemically aggressive samples can interact with the gasket material of the DAC chamber, and even with the diamond anvils, and this effect usually intensifies at high temperature and pressure. Consequently, both the sample and the high-pressure device can be affected. The erosion caused by an aggressive liquid can be considerably slowed down by its crystallization, which freezes the diffusion of molecules into the gasket. For example, *in situ* crystallization of halogen derivatives of acetic acid could only be performed in a DAC chamber with tungsten gaskets (Gajda & Katrusiak, 2009). In these experiments, the gasket was gradually eroded by the acid, but after its crystal-

lization the measurements could be performed over several days. In order fully to prevent erosion of the gasket, it can be coated with a layer of inert material, for example gold or platinum. Alternatively, a composite chamber can be prepared: after pre-indenting the gasket and drilling a hole at the centre of the indentation, a piece of gold wire can be fitted to the hole, and after pressing into a hole in the DAC again, a smaller hole can be drilled through this inset. A DAC chamber formed in this way has a gold lining and can be resistant to aggressive compounds.

2.7.13. High-pressure neutron diffraction

Neutron scattering is an indispensable and complementary technique in materials research (see Chapter 2.3), particularly for compounds containing heavy elements that strongly absorb X-rays, or light-atom weak X-ray scatterers (*e.g.* see Goncharenko & Loubeyre, 2005). However, the flux of neutron sources, both reactors and spallation targets, is several orders of magnitude lower than that of X-rays, even from traditional sealed X-ray tubes. Moreover, the scattering cross sections of neutrons are on average two orders of magnitude smaller than for X-rays (Bacon, 1975). These two considerations conflict with the requirement of small sample volume preferred for high-pressure devices. Consequently, a prohibitively long measurement time would be required to obtain meaningful neutron diffraction data from the DAC in its original form and size-optimized for X-ray studies. Therefore, initially, the designs of high-pressure devices for neutron scattering studies were based on typical large-volume presses: gas bombs with external multi-stage pressure generators, and piston-and-cylinder, multi-anvil and belt presses (Worlton & Decker, 1968; Bloch *et al.*, 1976; McWhan *et al.*, 1974; Srinivasa *et al.*, 1977; Besson, 1997; Klotz, 2012). The sample volume in the Bridgman-type opposed-anvil press, with flat anvils separated by a gasket of pipestone, was increased severalfold by making a recess at the centre of the pressure chamber of the so-called Chechevitsa anvils (Stishov & Popova, 1961*a*,*b*). The sample volume was further increased in toroid anvils by grooves supporting the gasket around the central recess (Khvostantsev *et al.*, 1977). This made them ideal for powder diffraction neutron measurements on samples of about 100 mm^3 to above 10 GPa in a Paris–Edinburgh hydraulic press (Besson *et al.*, 1992; Besson, 1997). The application of sintered diamond anvils increased this pressure range. High-pressure cells in a form optimized for neutron diffraction can contain between several cubic millimetres and a few cubic centimetres of sample volume. Such a large sample volume naturally limits the pressure range of cells used for neutron diffraction, compared with the DAC used for X-rays. However, the pressure range has increased considerably for neutron diffraction experiments during recent decades, to over 20 GPa in a moissanite anvil cell (Xu *et al.*, 2004; Dinga *et al.*, 2005), and to 40 GPa in a high-pressure cell capable of operating in helium cryostats at 0.1 K and in magnetic fields up to 7.5 T (Goncharenko, 2006; Goncharenko *et al.*, 1995). High-pressure high-temperature cells for neutron diffraction are usually equipped with internal heaters capable of exceeding 1500 K (Zhao *et al.*, 1999, 2000; Le Godec *et al.*, 2001, 2002).

It is particularly advantageous for the construction of large presses for neutron studies that most of the materials used have very low absorption of neutrons. There are also metals (vanadium, aluminium) with very low scattering lengths, and it is possible to obtain alloys ($Ti_{66}Zr_{34}$) with the scattering length scaled to zero. This allows access of the neutron beam to the sample and exit of reflections. In a Paris–Edinburgh cell operating in the time-of-flight mode, the incident beam enters the pressure chamber through the tungsten carbide anvil, along its axis, and the reflections leave the chamber through the gasket along the slit between the anvils with approximately $\pm 6^\circ$ opening (Besson *et al.*, 1992; Takahashi *et al.*, 1996). In this operation mode, highly neutron-absorbing anvils made of sintered cubic boron nitride (cBN) can also be used (Klotz, 2012). Alternatively, the monochromatic angle-dispersive mode of operation, with the incident and diffracted beams passing through the slit between the anvils, is possible but it is less efficient with regard to the use of the full spectrum of neutrons. The application of a focused neutron beam and the time-of-flight technique allow the use of small sample volumes of a fraction of a cubic millimetre in compact opposed-anvil high-pressure cells (Okuchi *et al.*, 2012). Two DACs were recently optimized for neutron diffraction on single crystals. Owing to the application of a white neutron beam, the structure of a crystal 0.005 mm^3 in volume was determined. All reflections could be recorded because of the smaller Merrill & Bassett (1974) design made of neutron-transparent beryllium–copper alloy (Binns *et al.*, 2016). Another design with a wide access to the sample for the primary and diffracted beams has been successfully used at a hot-neutron source (Grzechnik *et al.*, 2018).

2.7.14. Pressure determination

Pressure determination inside a high-pressure sample chamber is most straightforward in piston-and-cylinder devices, where the force applied to the piston and its surface area are known. Pressure is the force per unit area, with corrections for the friction between the cylinder wall and the piston (particularly significant above 1 GPa) and for the buoyancy of the piston, marginally important for all high pressures. Several types of mechanical pressure gauge are available. In the Bourdon gauge, a spiral metal tube that is pressurized inside unwinds and moves a pointer around a precise scale. Electrical resistance gauges are most often based on a manganin alloy sensor. The resistance of manganin changes at the rate of 2.4×10^{-5} GPa^{-1}, although precise calibration depends on the alloy composition and it changes with the age of the sensor. The resistance of manganin depends only very weakly on temperature.

The most common pressure calibration method used for the DAC is the fluorescence pressure scale of the ruby R_1 (λ_{R1} at 0.1 MPa is the reference; $\lambda_0 = 694.2$ nm) and R_2 (at 0.1 MPa, $\lambda_{R2} = 692.8$ nm) lines (Forman *et al.*, 1972; Barnett *et al.*, 1973; Syassen, 2008; Gao & Li, 2012). Synthetic ruby with a Cr^{3+} concentration of 3000–5500 p.p.m., illuminated with green laser light, is commonly used. Inclusions of spinels make natural ruby unsuitable as a pressure gauge. A piece of ruby is usually crushed into small pieces and one or several small chips are placed in the DAC chamber close to the sample (Hazen & Finger, 1982). Alternatively, small ruby spheres can be used for this purpose (Chervin *et al.*, 2001).

The linear pressure dependence of the ruby R_1 fluorescence line was established according to the equation of state (EOS) of NaCl to 19.5 GPa:

$$P\,(\mathrm{GPa}) = 2.74\Delta\lambda\,(\mathrm{nm}),$$

where $\Delta\lambda = \lambda_{R1} - \lambda_0$ (Piermarini *et al.*, 1975). The extension of the pressure range to 180 GPa, according to the equations of state of copper, gold and other metals, showed that $P(\Delta\lambda)$ is quasi-linear:

Table 2.7.2
Luminescence pressure sensors, their electronic transition types (s = singlet, d = doublet) and rates of spectral shifts (after Holzapfel, 1997)

Sensor	Transition	λ_0 (Å)	$d\lambda/dP$ (Å GPa^{-1})	$d\lambda/dT$ ($\times 10^{-2}$ Å K^{-1})	$(d\lambda/dP)/\Gamma$ (Å GPa^{-1})	$(d\lambda/dT)/(d\lambda/dP)$ ($\times 10^{-2}$ GPa K^{-1})
Cr^{3+}:Al_2O_3	$^2E\downarrow{}^4A_2$/d	6942	3.65 (9)	6.2 (3)	4.9	17.0
Sm^{2+}:SrB_4O_7	$^5D_0\downarrow{}^7F_0$/s	6854	2.55	−0.1	17.0	−0.4
Sm^{2+}:BaFCl	$^5D_0\downarrow{}^7F_0$/s	6876	11.0	−1.6	4.8	−1.5
Sm^{2+}:SrFCl	$^5D_0\downarrow{}^7F_0$/s	6903	11.2 (3)	−2.36 (3)	5.8	−2.1
Eu^{3+}:LaOCl	$^5D_0\downarrow{}^7F_0$/s	5787	2.5	−0.5	1.0	−2.0
Eu^{3+}:YAG	$^5D_0\downarrow{}^7F_1$/d	5906	1.97	−0.5	0.7	−2.5

Table 2.7.3
Parameters recommended for pressure determination by EOS measurements

Various face-centred cubic (f.c.c.) and body-centred cubic (b.c.c.) metals are used as calibrants, with the EOS given by equation (2.7.1) and the reference temperature T_R = 300 K (after Holzapfel, 1997).

Metal	a_{0R} (pm)	K_{0R} (GPa)	K'_{0R}	α_{0R} ($\times 10^6$ K)	$\delta_{\alpha R}$
Al	404.98 (1)	72.5 (4)	4.8 (2)	23.0 (4)	5.5 (11)
Cu	361.55 (1)	133.2 (2)	5.4 (2)	16.6 (3)	6.1 (6)
Ag	408.62 (1)	101.0 (2)	6.2 (2)	19.2 (4)	7.1 (6)
Au	407.84 (1)	166.7 (2)	6.3 (2)	14.2 (2)	7.2 (6)
Pd	388.99 (1)	189 (3)	5.3 (2)	11.6 (4)	6.0 (11)
Pt	392.32 (1)	277 (5)	5.2 (2)	8.9 (4)	5.9 (l1)
Mo	314.73 (1)	261 (5)	4.5 (5)	5.0 (4)	5.2 (14)
W	316.47 (1)	308 (2)	4.0 (2)	4.5 (4)	4.7 (11)

Table 2.7.4
Pressure fixed points at ambient temperature (after Holzapfel, 1997; Hall, 1980)

P (GPa)	Element transition
0.7569 (2)†	Hg freezing at 273 K
1.2 (1)†	Hg freezing at 298 K
2.55 (6)†	Bi I–II at 298 K
3.67 (3)†	Tl h.c.p.–f.c.c.
2.40 (10)†	Cs I–II
4.25 (1)†	Cs II–III
4.30 (1)†	Cs III–IV
5.5 (1)‡	Ba I–II
7.7 (2)‡	Bi III–IV
9.4 (3)†	Sn I–II
12.3 (5)†	Ba II–III
13.4 (6)†	Pb I–II

† Onset of forward transition. ‡ Centre of hysteresis.

$$P = 1904[(\lambda/\lambda_0)^B - 1]/B,$$

where B = 7.665 for quasi-hydrostatic and 5.0 for non-hydrostatic conditions (Mao *et al.*, 1986, 1978; Bell *et al.*, 1986).

The ruby fluorescence depends strongly on temperature (Barnett *et al.*, 1973; Vos & Schouten, 1991; Yamaoka *et al.*, 2012) and a temperature change of about 6 K causes R_1 line shifts equivalent to 0.1 GPa. The fluorescence-line dependence on temperature is much weaker for Sm^{2+}:SrB_4O_7 (Lacam & Chateau, 1989; Lacam, 1990; Datchi *et al.*, 1997) and the other rare-earth-doped sensors listed in Table 2.7.2. These sensors can be more sensitive to pressure than ruby, and together with ruby can be used simultaneously for both temperature and pressure calibration.

The calibration of most pressure gauges is based on comparisons of theoretical and shock-wave data (Holzapfel, 1997), so the derived equations of state are used with an accuracy of about 5% up to 1 TPa. The EOS recommended by Holzapfel (1997) is

$$P = [3K_0(1-x)/x^5]\exp[c_0(1-x)], \qquad (2.7.1)$$

where $x = a/a_0 = (V/V_0)^{1/3}$, $c_0 = 3(K_0' - 3)/2$, a is the unit-cell dimension, V is the unit-cell volume, a_{0R} and V_{0R} are the reference parameters under ambient conditions (Table 2.7.3), α_{0R} is the thermal expansion coefficient, K_{0R} is the bulk modulus, and $K_0' = dK_0/dP$. $dK_0/dT = -3\alpha_{0R}K_0\delta_{\alpha R}$, where $\delta_{\alpha R} = \partial(\ln\alpha)/\partial(\ln V)_{TR}$. Pressure can be computed by assuming constant K_0' and linear temperature relations for T close to or higher than T_R = 300 K:

$$a_0(T) = a_{0R}[1 + \alpha_{0R}(T - T_R)],$$
$$V_0(T) = V_{0R}[1 + 3\alpha_{0R}(T - T_R)],$$
$$K_0(T) = K_{0R}[1 - \alpha_{0R}\delta_{\alpha R}(T - T_R)].$$

The details of the parameterization are explained by Holzapfel (1991, 1994) and listed for the simple face-centred (f.c.c.) and body-centred (b.c.c.) cubic metals in Table 2.7.3 (Holzapfel, 1997). Powders of these metals can be mixed with the sample and its pressure can be calibrated according to the unit-cell dimension of the standard. The well known compressibilities of NaCl, CaF_2 and MgO, in the form of either powders or single crystals, are also often used as internal pressure standards (Dorfman *et al.*, 2010, 2012; Dorogokupets & Dewaele, 2007).

An independent pressure assessment can be obtained from standard materials undergoing pressure-induced phase transitions (Table 2.7.4). This method is limited to just a few pressure points (Holzapfel, 1997), but they can provide a useful verification of other pressure gauges.

Other methods of pressure calibration are still being developed. For example, it has been shown that very high pressure can be determined from the Raman shift of strained diamond-anvil culets (Akahama & Kawamura, 2004). The strong piezochromic effect of visible colour changes in soft coordination polymers allows pressure calibration without spectrometers. These changes can proceed gradually (Andrzejewski & Katrusiak, 2017*a*) and abruptly at phase transitions (Andrzejewski & Katrusiak, 2017*b*). Another method of pressure calibration is based on the luminescence lifetime of lanthanide nanocrystals (Runowski *et al.*, 2017).

2.7.15. High-pressure diffraction data corrections

Apart from the Lorentz and polarization (Lp) corrections routinely applied to reflection intensities measured for bare crystals (*i.e.* crystals not enclosed in environment devices), as well as other corrections like extinction and absorption in the sample, the effects of the high-pressure cell should additionally be accounted for. These effects mainly include absorption in the pressure-vessel walls, shadowing of the sample by the pressure-cell opaque elements and elimination of the reflections of the diamond anvils for measurements in a DAC. The set of corrections is usually described for the specific pressure vessel. For a

typical DAC with the anvils (about 1.7 mm high) supported directly on the edges of conical steel or tungsten carbide windows, and for Mo *K* radiation, the absorption is quite uniform and varies between about 0.50 and 0.60, for the beams passing close to the DAC axis and those close to the conical window edge, respectively. This absorption is even smaller at the shorter wavelengths used for high-pressure X-ray diffraction studies at synchrotrons. For this reason the absorption correction for the DAC is often neglected.

The sample-shadowing correction accounts for the loss of intensity due to the sample being partly shadowed by the gasket edges. This effect can be avoided by choosing a sufficiently small crystal or by applying a sufficiently narrow beam, which would illuminate only the central part of the sample. Such microbeams are now routinely used at synchrotrons. For these reasons, synchrotron data are often used straightforwardly after applying just the Lp corrections and incident-beam variation and eliminating the diamond reflections. In fact there are very few diamond reflections because of the small unit cell and many systematic absences, and the DAC can be treated as a low-background cuvette for powder diffraction.

The corrections for absorption and gasket shadowing are very important for high-pressure data collection in the laboratory, where a sealed X-ray tube is used. Its beam is relatively weak and for this reason the quality of the data (signal-to-background ratio) is low, but can be improved by increasing the sample volume. Ideally, a sample that completely fills the DAC chamber secures the highest intensity of reflections. However, for large samples the shadowing of the incident and diffracted beams by the gasket is very significant and should be corrected for (Katrusiak, 2004*a*,*b*).

The calculation of the so-called analytical corrections, obtained by dividing the high-pressure chamber into small pixels and calculating the beam's trajectory to and off each pixel, through all the DAC components (beryllium discs, if present, diamond anvils, hydrostatic fluid and sample) can precisely eliminate errors. Having the correct reflection intensities simplifies the structure solution of new phases and increases the accuracy of the refined structure. It has been shown that some incompleteness of accurate data does not cause systematic errors in the structural parameters (Dziubek & Katrusiak, 2002). In most calculations of reflection intensity corrections, the cylindrical symmetry of the DAC about its axis is assumed (Katrusiak, 2001, 2004*a*,*b*; Hazen & Finger, 1982; Angel, 2004; Kuhs *et al.*, 1996; Miletich *et al.*, 2000).

Diffraction measurements with area detectors have the advantage of collecting data with a considerable redundancy factor, which is often routinely used to calculate the so-called empirical absorption corrections, which are sometimes applied to a sample in a DAC. The intensities of powder diffraction reflections measured at synchrotrons with microbeams are often not corrected, particularly when the DAC axis is not significantly moved from the primary beam during data collection. The redundancy of the data also considerably reduces the effect of simultaneous diffraction events by the sample and one or two of the diamond anvils.

The most significant systematic errors in the diffraction of a sample in a DAC may be due to preferential orientation of the grains, which can occur for an anisotropic sample and non-hydrostatic conditions in the chamber. This effect can be accounted for in the process of Rietveld refinement (McMahon, 2004; Filinchuk, 2010), or may require repetition of the measurement after reloading a new sample into the DAC.

2.7.16. Final remarks

During the last 100 years, and particularly during the last few decades, high-pressure diffractometric techniques have been developed covering a broad range of research in different fields of science. It is simply impossible to present all aspects of high-pressure methodology in one chapter. Many books, book chapters and scientific papers have been written on high-pressure research and therefore I have chosen to present a 'flavour' of high-pressure crystallography, rather than concentrating on all its aspects. Readers interested in specific subjects can find the required information in a number of instructive books (Hazen & Finger, 1982; Eremets, 1996; Holzapfel, 1997; Katrusiak & McMillan, 2004; Boldyreva & Dera, 2010; McMahon, 2012) and in numerous articles in research journals. This chapter is only an introduction and gives some useful reference information for high-pressure crystallographers.

It should be stressed that the sample-preparation techniques for high-pressure studies are relatively demanding. Therefore, diffraction studies are often 'adjusted' to the form of the sample obtained in the high-pressure device. In particular, powder diffraction, single-crystal and spectroscopic measurements can be conducted on some synchrotron beamlines (see *e.g.* Dera *et al.*, 2013). Many experimental techniques complementary to high-pressure crystallographic studies have not been mentioned here.

It can be concluded that, over the years, high-pressure research has become quite popular in materials science and at present all over the world there are hundreds or even thousands of scientists capable of performing high-pressure experiments. Their scientific output is significant, and can be used as a guide for those interested in specific types of high-pressure research.

References

Abrahams, S. C., Collin, R. L., Lipscomb, W. N. & Reed, T. B. (1950). *Further techniques in single-crystal X-ray diffraction studies at low temperatures. Rev. Sci. Instrum.* **21**, 396–397.

Adams, D. M. & Christy, A. G. (1992). *Materials for high-temperature diamond-anvil cells. High Press. Res.* **8**, 685–689.

Ahrens, T. J. (1980). *Dynamic compression of Earth materials. Science*, **207**, 1035–1041.

Ahrens, T. J. (1987). *Shock wave techniques for geophysics and planetary physics.* In *Methods of Experimental Physics*, Vol. 24A, edited by C. G. Sammis & T. L. Henyey, pp. 185–235. New York: Academic Press.

Ahsbahs, H. (2004). *New pressure cell for single-crystal X-ray investigations on diffractometers with area detectors. Z. Kristallogr.* **219**, 305–308.

Akahama, Y., Hirao, N., Ohishi, Y. & Singh, A. K. (2014). *Equation of state of bcc-Mo by static volume compression to 410 GPa. J. Appl. Phys.* **116**, 223504.

Akahama, Y. & Kawamura, H. (2004). *High-pressure Raman spectroscopy of diamond anvils to 250 GPa: method for pressure determination in the multimegabar pressure range. J. Appl. Phys.* **96**, 3748–3751.

Akahama, Y. & Kawamura, H. (2010). *Pressure calibration of diamond anvil Raman gauge to 410 GPa. J. Phys. Conf. Ser.* **215**, 012195.

Akimoto, S., Suzuki, T., Yagi, T. & Shimomura, O. (1987). *Phase diagram of iron determined by high-pressure/temperature X-ray diffraction using synchrotron radiation*. In *High-Pressure Research in Mineral Physics*, Geophysics Monograph Series, Vol. 39, edited by M. H. Manghnani & Y. Syono, pp. 149–154. Washington, DC: AGU.

Alireza, P. L. & Lonzarich, G. G. (2009). *Miniature anvil cell for high-pressure measurements in a commercial superconducting quantum interference device magnetometer. Rev. Sci. Instrum.* **80**, 023906.

Allan, D. R. & Clark, S. J. (1999). *Impeded dimer formation in the high-pressure crystal structure of formic acid. Phys. Rev. Lett.* **82**, 3464–3467.

Andrzejewski, M. & Katrusiak, A. (2017*a*). *Piezochromic porous metal–organic framework. J. Phys. Chem. Lett.* **8**, 279–284.

Andrzejewski, M. &. Katrusiak, A. (2017*b*). *Piezochromic topology switch in a coordination polymer. J. Phys. Chem. Lett.* **8**, 929–935.

Andrzejewski, M., Olejniczak, A. & Katrusiak, A. (2011). *Humidity control of isostructural dehydration and pressure-induced polymorphism in 1,4-diazabicyclo[2.2.2]octane dihydrobromide monohydrate. Cryst. Growth Des.* **11**, 4892–4899.

Angel, R. J. (2004). *Absorption corrections for diamond-anvil pressure cells implemented in the software package Absorb6.0. J. Appl. Cryst.* **37**, 486–492.

Angel, R. J., Bujak, M., Zhao, J., Gatta, G. D. & Jacobsen, S. D. (2007). *Effective hydrostatic limits of pressure media for high-pressure crystallographic studies. J. Appl. Cryst.* **40**, 26–32.

Bacon, G. E. (1975). *Neutron Diffraction*. Oxford University Press.

Baranowski, B. & Bujnowski, W. (1970). *A device for generation of hydrogen pressure to 25000 at. Ann. Soc. Chim. Polonarum*, **44**, 2271–2273.

Barnett, J. D., Block, S. & Piermarini, G. J. (1973). *An optical fluorescence system for quantitative pressure measurement in the diamond-anvil cell. Rev. Sci. Instrum.* **44**, 1–9.

Bassett, W. A. (2001). *The birth and development of laser heating in diamond anvil cells. Rev. Sci. Instrum.* **72**, 1270–1272.

Bassett, W. A. (2009). *Diamond anvil cell, 50th birthday. High Press. Res*. **29**, 163–186.

Bassett, W. A., Shen, A. H., Bucknum, M. & Chou, I.-M. (1993). *A new diamond anvil cell for hydrothermal studies to 2.5 GPa and from −190 to 1200˚C. Rev. Sci. Instrum.* **64**, 2340–2345.

Bassett, W. A. & Takahashi, T. (1965). *Silver iodide polymorphs. Am. Mineral*. **50**, 1576–1594.

Batsanov, S. S. (2004). *Solid phase transformations under high dynamic pressure.* In *High-Pressure Crystallography*, edited by A. Katrusiak & P. F. McMillan, pp. 353–366. Dordrecht: Kluwer.

Baublitz, M. A., Arnold, V. & Ruoff, A. L. (1981). *Energy dispersive X-ray diffraction from high pressure polycrystalline specimens using synchrotron radiation. Rev. Sci. Instrum.* **52**, 1616–1624.

Bell, P. M. & Mao, H.-K. (1981). *Degree of hydrostaticity in He, Ne, and Ar pressure-transmitting media. Carnegie Inst. Washington Yearb.* **80**, 404–406.

Bell, P. M., Xu, J. A. & Mao, H.-K. (1986). *Static compression of gold and copper and calibration of the ruby pressure scale to pressures to 1.8 megabars.* In *Shock Waves in Condensed Matter*, edited by Y. M. Gupta, pp. 125–130. New York: Plenum Press.

Besson, J. M. (1997). *Pressure generation.* In *High-Pressure Techniques in Chemistry and Physics. A Practical Approach*, edited by W. B. Holzapfel & N. S. Isaacs, pp. 1–45. Oxford University Press.

Besson, J. M., Nelmes, R. J., Hamel, G., Loveday, J. S., Weill, G. & Hull, S. (1992). *Neutron powder diffraction above 10 GPa. Physica B*, **180–181**, 907–910.

Binns, J., Kamenev, K. V., McIntyre, G. J., Moggach, S. A. & Parsons, S. (2016). *Use of a miniature diamond-anvil cell in high-pressure single-crystal neutron Laue diffraction. IUCrJ*, **3**, 168–179.

Blaschko, O. & Ernst, G. (1974). *Autofrettaged high pressure chamber for use in inelastic neutron scattering. Rev. Sci. Instrum.* **45**, 526–528.

Bloch, D., Paureau, J., Voiron, J. & Parisot, G. (1976). *Neutron scattering at high pressure. Rev. Sci. Instrum.* **47**, 296–298.

Boehler, R. & De Hantsetters, K. (2004). *New anvil designs in diamond-cells. High Press. Res*. **24**, 391–396.

Boehler, R., Nicol, M., Zha, C. S. & Jonson, M. L. (1986). *Resistance heating of Fe and W in diamond anvil cells. Physica B*, **139–140**, 916–918.

Boehler, R., Ross, M. P. & Boercker, D. B. (2001). *High-pressure melting curves of argon, krypton, and xenon: deviation from corresponding states theory. Phys. Rev. Lett*. **86**, 5731–5734.

Boldyreva, E. V. (2010). *High-pressure studies of pharmaceuticals and biomimetics. Fundamentals and applications. A general introduction.* In *High-Pressure Crystallography. From Fundamental Phenomena to Technological Applications*, edited by E. Boldyreva & P. Dera, pp. 533–543. Dordrecht: Springer.

Boldyreva, E. V. & Dera, P. (2010). Editors. *High-Pressure Crystallography: From Fundamental Phenomena to Technological Applications*. Dordrecht: Springer.

Boldyreva, E. V., Dmitriev, V. P. & Hancock, B. C. (2006). *Effect of pressure up to 5.5 GPa on dry powder samples of chlorpropamide form-A. Int. J. Pharm.* **327**, 51–57.

Boldyreva, E. V., Shakhtshneider, T. P., Ahsbahs, H., Sowa, H. & Uchtmann, H. (2002). *Effect of high pressure on the polymorphs of paracetamol. J. Therm. Anal. Cal.* **68**, 437–452.

Bridgman, P. W. (1914). *The coagulation of albumen by pressure. J. Biol. Chem.* **19**, 511–512.

Bridgman, P. W. (1935). *Effects of high shearing stress combined with high hydrostatic pressure. Phys. Rev.* **48**, 825–847.

Bridgman, P. W. (1941). *Explorations toward the limit of utilizable pressures. J. Appl. Phys.* **12**, 461–469.

Bridgman, P. W. (1952). *The resistance of 72 elements, alloys and compounds to 100,000 kg/cm^2. Proc. Am. Acad. Arts Sci.* **81**, 167–251.

Bridgman, P. W. (1964). *Collected Experimental Papers*, Volumes I–VII. Cambridge, MA: Harvard University Press.

Brister, K. E., Vohra, Y. K. & Ruoff, A. L. (1986). *Microcollimated energy-dispersive X-ray diffraction apparatus for studies at megabar pressures with a synchrotron source. Rev. Sci. Instrum.* **57**, 2560–2563.

Budzianowski, A. & Katrusiak, A. (2004). *High-pressure crystallographic experiments with a CCD detector.* In *High-Pressure Crystallography*, edited by A. Katrusiak & P. F. McMillan, pp. 101–112. Dordrecht: Kluwer.

Budzianowski, A. & Katrusiak, A. (2006*a*). *Pressure tuning between NH···N hydrogen-bonded ice analogue and NH···Br polar dabcoHBr complexes. J. Phys. Chem. B*, **110**, 9755–9758.

Budzianowski, A. & Katrusiak, A. (2006*b*). *Pressure-frozen benzene I revisited. Acta Cryst.* B**62**, 94–101.

Bujak, M., Budzianowski, A. & Katrusiak, A. (2004). *High-pressure in-situ crystallization, structure and phase transitions in 1,2-dichloroethane. Z. Kristallogr.* **219**, 573–579.

Bujak, M., Podsiadło, M. & Katrusiak, A. (2008). *Energetics of conformational conversion between 1,1,2-trichloroethane polymorphs. Chem. Commun.* pp. 4439–4441.

Buras, B., Olsen, J. S. & Gerward, L. (1977). *White beam, X-ray, energy-dispersive diffractometry using synchrotron radiation. Nucl. Instrum. Methods*, **152**, 293–296.

Buras, B., Olsen, J. S., Gerward, L., Will, G. & Hinze, E. (1977). *X-ray energy-dispersive diffractometry using synchrotron radiation. J. Appl. Cryst.* **10**, 431–438.

Bureau, H., Burchard, M., Kubsky, S., Henry, S., Gonde, C., Zaitsev, A. & Meijer, J. (2006). *Intelligent anvils applied to experimental investigations: state of the art. High Press. Res*. **26**, 251–265.

Busing, W. R. & Levy, H. A. (1967). *Angle calculations for 3- and 4-circle X-ray and neutron diffractometers. Acta Cryst.* **22**, 457–464.

Chervin, J. C., Canny, B., Besson, J. M. & Pruzan, Ph. (1995). *A diamond anvil cell for IR microspectroscopy. Rev. Sci. Instrum.* **66**, 2595–2598.

Chervin, J. C., Canny, B. & Mancinelli, M. (2001). *Ruby-spheres as pressure gauge for optically transparent high pressure cells. High Press. Res*. **21**, 305–314.

Cohen, W. M. (1933). *X-ray investigations at high pressures. Phys. Rev.* **44**, 326–327.

Couzinet, B., Dahan, N., Hamel, G. & Chervin, J.-C. (2003). *Optically monitored high-pressure gas loading apparatus for diamond anvil cells. High Press. Res.* **23**, 409–415.

Crichton, W. A. & Mezouar, M. (2004). *Methods and application of the Paris–Edinburgh press to X-ray diffraction structure solution with large-volume samples at high pressures and temperatures.* In *Advances in High-Pressure Technology for Geophysical Applications*, edited by J. Chen, Y. Wang, T. S. Duffy, G. Shen & L. F. Dobrzhinetskaya, pp. 353–369. Amsterdam: Elsevier.

Dalladay-Simpson, P., Howie, R. T. & Gregoryanz, E. (2016). *Evidence for a new phase of dense hydrogen above 325 gigapascals. Nature*, **529**, 63–67.

Datchi, F., LeToullec, R. & Loubeyre, P. (1997). *Improved calibration of the SrB_4O_7:Sm^{2+} optical pressure gauge: advantages at very high pressures and high temperatures. J. Appl. Phys.* **81**, 3333–3339.

Denner, W., Schulz, H. & d'Amour, H. (1978). *A new measuring procedure for data collection with a high-pressure cell on an X-ray four-circle diffractometer. J. Appl. Cryst.* **11**, 260–264.

Dera, P. & Katrusiak, A. (1999). *Diffractometric crystal centering. J. Appl. Cryst.* **32**, 510–515.

Dera, P., Zhuravlev, K., Prakapenka, V., Rivers, M. L., Finkelstein, G. F., Grubor-Urosevic, O., Tschauner, O., Clark, S. M. & Downs, R. T. (2013). *High pressure single-crystal micro X-ray diffraction analysis with GSE_ADA/RSV software. High Press. Res*. **33**, 466–484.

Dewaele, A. & Loubeyre, P. (2007). *Pressurizing conditions in helium-pressure-transmitting medium. High. Press. Res.* **27**, 419–429.

Dewaele, A., Loubeyre, P., Florent Occelli, F., Marie O. & Mezouar, M. (2018). *Toroidal diamond anvil cell for detailed measurements under extreme static pressures. Nat. Commun.* **9**, 2913.

Dinga, Y., Xu, J., Prewitt, Ch. T., Hemley, R. J., Mao, H., Cowan, J. A., Zhang, J., Qian, J., Vogel, S. C., Lokshin, K. & Zhao, Y. (2005). *Variable pressure–temperature neutron diffraction of wüstite, $Fe_{1-x}O$: absence of long-range magnetic order to 20 GPa. Appl. Phys. Lett.* **86**, 052505.

Dorfman, S. M., Jiang, F., Mao, Z., Kubo, A., Meng, Y., Prakapenka, V. B. & Duffy, T. S. (2010). *Phase transitions and equations of state of alkaline earth fluorides CaF_2, SrF_2, and BaF_2 to Mbar pressures. Phys. Rev. B*, **81**, 174121.

Dorfman, S. M., Prakapenka, V. B., Meng, Y. & Duffy, T. S. (2012). *Intercomparison of pressure standards (Au, Pt, Mo, MgO, NaCl and Ne) to 2.5 Mbar. J. Geophys. Res.* **117**, B08210.

Dorogokupets, P. I. & Dewaele, A. (2007). *Equations of state of MgO, Au, Pt, NaCl-B1, and NaCl-B2: internally consistent high-temperature pressure scales. High Press. Res*. **27**, 431–446.

Dubrovinskaia, N. & Dubrovinsky, L. S. (2003). *Whole-cell heater for the diamond anvil cell. Rev. Sci. Instrum.* **74**, 3433–3437.

Dubrovinskaia, N., Dubrovinsky, L., Solopova, N. A., Abakumov, A., Turner, S., Hanfland, M., Bykova, E., Bykov, M., Prescher, C., Prakapenka, V. B., Petitgirard, S., Chuvashova, I., Gasharova, B., Mathis, Y.-L., Ershov, P., Snigireva, I. & Snigirev, A. (2016). *Terapascal static pressure generation with ultrahigh yield strength nanodiamond. Sci. Adv.* **2**, e1600341.

Dubrovinsky, L., Dubrovinskaia, N., Prakapenka, V. B. & Abakumov, A. M. (2012). *Implementation of micro-ball nanodiamond anvils for high-pressure studies above 6 Mbar. Nat. Commun.* **3**, 1163.

Dubrovinsky, L. S., Saxena, S. K. & Lazor, P. (1998). *High-pressure and high-temperature in situ X-ray diffraction study of iron and corundum to 68 GPa using an internally heated diamond anvil cell. Phys. Chem. Miner.* **25**, 434–441.

Dziubek, K. & Katrusiak, A. (2002). *Structural refinements on restricted intensity data collected in high-pressure diffraction experiments. Defect Diffus. Forum*, **208–209**, 319–322.

Dziubek, K. F. & Katrusiak, A. (2004). *Compression of intermolecular interactions in CS_2 crystal. J. Phys. Chem. B*, **108**, 19089–19092.

Dziubek, K. F. & Katrusiak, A. (2014). *Complementing diffraction data with volumetric measurements. Z. Kristallogr.* **229**, 129–134.

Dziubek, K., Podsiadło, M. & Katrusiak, A. (2007). *Nearly isostructural polymorphs of ethynylbenzene: resolution of $\equiv CH\cdots\pi$(arene) and cooperative $\equiv CH\cdots\pi(C\equiv C)$ interactions by pressure freezing. J. Am. Chem. Soc.* **129**, 12620–12621.

Eggert, J. H., Xu, L. W., Che, R. Z., Chen, L. C. & Wang, J. F. (1992). *High pressure refractive-index measurements of 4/1 methanol–ethanol. J. Appl. Phys.* **72**, 2453–2461.

Eremets, M. (1996). *High Pressure Experimental Methods*. New York: Oxford University Press.

Fabbiani, F. P. A. (2010). *New frontiers in physical form discovery: high-pressure recrystallization of pharmaceutical and other molecular compounds.* In *High-Pressure Crystallography. From Fundamental Phenomena to Technological Applications*, edited by E. Boldyreva & P. Dera, pp. 545–558. Dordrecht: Springer.

Fabbiani, F. P. A., Allan, D. R., David, W. I. F., Moggach, S. A., Parsons, S. & Pulham, C. R. (2004). *High-pressure recrystallization – a route to new polymorphs and solvates. CrystEngComm*, **6**, 504–511.

Fabbiani, F. P. A., Allan, D. R., Parsons, S. & Pulham, C. R. (2005). *An exploration of the polymorphism of piracetam using high pressure. CrystEngComm*, **7**, 179–186.

Fabbiani, F. P. A., Dittrich, B., Florence, A. J., Gelbrich, T., Hursthouse, M. B., Kuhs, W. F., Shankland, N. & Sowa, H. (2009). *Crystal structures with a challenge: high-pressure crystallisation of ciprofloxacin sodium salts and their recovery to ambient pressure. CrystEngComm*, **11**, 1396–1406.

Fabbiani, F. P. A. & Pulham, C. R. (2006). *High-pressure studies of pharmaceutical compounds and energetic materials. Chem. Soc. Rev.* **35**, 932–942.

Fei, Y. & Wang, Y. (2000). *High-pressure and high-temperature powder diffraction. Rev. Mineral. Geochem.* **41**, 521–557.

Filinchuk, Y. (2010). *Light metal hydrates under non-ambient conditions: probing chemistry by diffraction?* In *High-Pressure Crystallography. From Fundamental Phenomena to Technological Applications*, edited by E. Boldyreva & P. Dera, pp. 281–291. Dordrecht: Springer.

Finger, L. W. & King, H. E. (1978). *A revised method of operation of the single-crystal diamond cell and refinement of the structure of NaCl at 32 kbar. Am. Mineral*. **63**, 337–342.

Fiquet, G. & Andrault, D. (1999). *Powder X-ray diffraction under extreme conditions of pressure and temperature. J. Synchrotron Rad.* **6**, 81–86.

Forman, R. A., Piermarini, G. J., Barnett, J. D. & Block, S. (1972). *Pressure measurement made by the utilization of ruby sharp-line luminescence. Science*, **176**, 284–285.

Fourme, R. (1968). *Appareillage pour études radiocristallographiques sous pression et à température variable. J. Appl. Cryst.* **1**, 23–30.

Fourme, R. E., Girard, R., Kahn, I., Ascone, M., Mezouar, T., Lin, J. E. & Johnson (2004). *State of the art and prospects of macromolecular X-ray crystallography at high hydrostatic pressure.* In *High-Pressure Crystallography*, edited by A. Katrusiak & P. F. McMillan, pp. 527–542. Dordrecht: Kluwer.

Gajda, R. & Katrusiak, A. (2009). *Electrostatic matching versus close-packing molecular arrangement in compressed dimethyl sulfoxide (DMSO) polymorphs. J. Phys. Chem. B*, **113**, 2436–2442.

Gao, R. & Li, H. (2012). *Pressure measurement using the R fluorescence peaks and 417 cm^{-1} Raman peak of an anvil in a sapphire-anvil cell. High Press. Res*. **32**, 176–185.

Giriat, G., Wang, W., Attfield, J. P., Huxley, A. D. & Kamenev, K. V. (2010). *Turnbuckle diamond anvil cell for high-pressure measurements in a superconducting quantum interference device magnetometer. Rev. Sci. Instrum.* **81**, 073905.

Goncharenko, I. N. (2004). *Magnetic properties of crystals and their studies at high pressure conditions.* In *High-Pressure Crystallography*, edited by A. Katrusiak & P. F. McMillan, pp. 321–340. Dordrecht: Kluwer.

Goncharenko, I. N. (2006). *Magnetic and crystal structures probed by neutrons in 40 GPa pressure range. Acta Cryst.* A**62**, s95.

Goncharenko, I. & Loubeyre, P. (2005). *Neutron and X-ray diffraction study of the broken symmetry phase transition in solid deuterium. Nature*, **435**, 1206–1209.

Goncharenko, I. N., Mignot, J.-M., Andre, G., Lavrova, O. A., Mirebeau, I. & Somenkov, V. A. (1995). *Neutron diffraction studies of magnetic structure and phase transitions at very high pressures. High Press. Res*. **14**, 41–53.

Goncharenko, I. N. & Mirebeau, I. (1998). *Magnetic neutron diffraction under very high pressures. Study of europium monochalcogenides. Rev. High Press. Sci. Technol*. **7**, 475–480.

Graf, D. E., Stillwell, R. L., Purcell, K. M. & Tozer, S. W. (2011). *Nonmetallic gasket and miniature plastic turnbuckle diamond anvil cell for pulsed magnetic field studies at cryogenic temperatures. High Press. Res*. **31**, 533–543.

Grocholski, B. & Jeanloz, R. (2005). *High-pressure and -temperature viscosity measurements of methanol and 4:1 methanol:ethanol solution. J. Chem. Phys.* **123**, 204503.

Gruner, S. M. (2004). *Soft materials and biomaterials under pressure.* In *High-Pressure Crystallography*, edited by A. Katrusiak & P. F. McMillan, pp. 543–556. Dordrecht: Kluwer.

Grzechnik, A., Meven, M. & Friese, K. (2018). *Single-crystal neutron diffraction in diamond anvil cells with hot neutrons. J. Appl. Cryst.* **51**, 351–356.

Guńka, P. A., Dziubek, K. F., Gładysiak, A., Dranka, M., Piechota, J., Hanfland, M., Katrusiak, A. & Zachara, J. (2015). *Compressed arsenolite As_4O_6 and its helium clathrate $As_4O_{62}He$. Cryst. Growth Des.* **15**, 3740–3745.

Hall, H. T. (1980). *High pressure techniques*. In *Chemical Experimentation under Extreme Conditions, Techniques of Chemistry*, Vol. IX, ch. II, edited by A. Weissberger & B. Rossiter, pp. 9–72. Chichester: John Wiley & Sons.

Hamilton, W. C. (1974). *International Tables for X-ray Crystallography*, Vol. IV, pp. 273–284. Birmingham: Kynoch Press.

Hammersley, A. P., Svensson, S. O., Hanfland, M., Fitch, A. N. & Hauessermann, D. (1996). *Two-dimensional detector systems. From real detector to idealised image of two-theta scan. High Press. Res.* **14**, 235–248.

Hanfland, M., Proctor, J. E., Guillaume, Ch. L., Degtyareva, O. & Gregoryanz, E. (2011). *High-pressure synthesis, amorphization, and decomposition of silane. Phys. Rev. Lett.* **106**, 095503.

Hazen, R. M. (1999). *The Diamond Makers*. Cambridge Unversity Press.

Hazen, R. M. & Finger, L. (1982). *Comparative Crystal Chemistry*. New York: John Wiley & Sons.

Holzapfel, W. B. (1991). *Equations of state for strong compression. High. Press. Res.* **7**, 290–292.

Holzapfel, W. B. (1994). *Approximate equations of state for solids from limited data sets. J. Phys. Chem. Solids*, **55**, 711–719.
Holzapfel, W. B. (1997). *Pressure determination.* In *High-Pressure Techniques in Chemistry and Physics. A Practical Approach*, edited by W. B. Holzapfel & N. S. Isaacs, pp. 47–55. Oxford University Press.
Huppertz, H. (2004). *Multianvil high-pressure/high-temperature synthesis in solid state chemistry. Z. Kristallogr*. **219**, 330–338.
Ivanov, A. N., Nikolaev, N. A., Pashkin, N. V., Savenko, B. N., Smirnov, L. S. & Taran, Y. V. (1995). *Ceramic high pressure cell with profiled anvils for neutron diffraction investigations (up to 7 GPa). High-Press. Res.* **14**, 203–208.
Jamieson, J. C., Lawson, A. W. & Nachtrieb, N. D. (1959). *New device for obtaining X-ray diffraction patterns from substances exposed to high pressure. Rev. Sci. Instrum.* **30**, 1016–1019.
Jenei, Zs., O'Bannon, E. F., Weir, S. T., Cynn, H., Lipp, M. J. & Evans, W. J. (2018). *Single crystal toroidal diamond anvils for high pressure experiments beyond 5 megabar. Nat. Commun.* **9**, 3563.
Jephcoat, A. P., Finger, L. W. & Cox, D. E. (1992). *High pressure, high resolution synchrotron X-ray powder diffraction with a position-sensitive detector. High Press. Res*. **8**, 667–676.
Katrusiak, A. (1999). *A hinge goniometer head. J. Appl. Cryst.* **32**, 576–578.
Katrusiak, A. (2001). *Absorption correction for crystal-environment attachments from direction cosines. Z. Kristallogr.* **216**, 646–647.
Katrusiak, A. (2004*a*). *Shadowing and absorption corrections of single-crystal high-pressure data. Z. Kristallogr.* **219**, 461–467.
Katrusiak, A. (2004*b*). *Shadowing and absorption corrections of high-pressure powder diffraction data: toward accurate electron-density determinations. Acta Cryst.* A**60**, 409–417.
Katrusiak, A. (2008). *High-pressure crystallography. Acta Cryst.* A**64**, 135–148.
Katrusiak, A. & Dauter, Z. (1996). *Compressibility of lysozyme protein crystals by X-ray diffraction. Acta Cryst.* D**52**, 607–608.
Katrusiak, A. & McMillan, P. F. (2004). Editors. *High Pressure Crystallography*. Dordrecht: Kluwer Academic Press.
Keller, K., Schlothauer, T., Schwarz, M., Heide, G. & Kroke, E. (2012). *Shock wave synthesis of aluminium nitride with rocksalt structure. High Press. Res.* **32**, 23–29.
Kenichi, T., Sahu, P. Ch., Yoshiyasu, K. & Yasuo, T. (2001). *Versatile gas-loading system for diamond-anvil cells. Rev. Sci. Instrum.* **72**, 3873–3876.
Khvostantsev, L. G. (1984). *A verkh-niz (up-down) device of toroid type for generation of high pressure. High Temp. High Press.* **16**, 165–169.
Khvostantsev, L. G., Slesarev, V. N. & Brazhkin, V. V. (2004). *Toroid type high-pressure device: history and prospects. High Press. Res*. **24**, 371–383.
Khvostantsev, L. G., Vereshchagin, L. F. & Novikov, A. P. (1977). *Device of toroid type for high pressure generation. High Temp. High Press.* **9**, 637–639.
King, H. E. & Finger, L. W. (1979). *Diffracted beam crystal centering and its application to high-pressure crystallography. J. Appl. Cryst.* **12**, 374–378.
Klotz, S. (2012). *Techniques in High Pressure Neutron Scattering*. Boca Raton: CRC Press.
Klotz, S., Chervin, J.-C., Munsch, P. & Le Marchand, G. (2009). *Hydrostatic limits of 11 pressure transmitting media. J. Phys. D Appl. Phys.* **42**, 075413.
Konno, M., Okamoto, T. & Shirotani, I. (1989). *Structure changes and proton transfer between O···O in bis(dimethylglyoximato)platinum(II) at low temperature (150 K) and at high pressures (2.39 and 3.14 GPa). Acta Cryst.* B**45**, 142–147.
Koster van Groos, A. F., Guggenheim, S. & Cornell, C. (2003). *Environmental chamber for powder X-ray diffractometers for use at elevated pressures and low temperatures. Rev. Sci. Instrum.* **74**, 273–275.
Kuhs, W. F., Bauer, F. C., Hausmann, R., Ahsbahs, H., Dorwarth, R. & Hölzer, K. (1996). *Single crystal diffraction with X-rays and neutrons: high quality at high pressure? High Press. Res.* **14**, 341–352.
Kundrot, C. E. & Richards, F. M. (1986). *Collection and processing of X-ray diffraction data from protein crystals at high pressure. J. Appl. Cryst.* **19**, 208–213.
Kunz, M. (2001). *High pressure phase transformations.* In *Phase Transformations in Materials*, edited by G. Kostorz, pp. 655–695. Weinheim: Wiley-VCH Verlag.
Lacam, A. (1990). *The SrB_4O_7:Sm^{2+} optical sensor and the pressure homogenization through thermal cycles in diamond anvil cells. High Press. Res*. **5**, 782–784.
Lacam, A. & Chateau, C. (1989). *High-pressure measurements at moderate temperatures in a diamond anvil cell with a new optical sensor: SrB_4O_7:Sm^{2+}. J. Appl. Phys.* **66**, 366–372.
Le Godec, Y., Dove, M. T., Francis, D. J., Kohn, S. C., Marshall, W. G., Pawley, A. R., Price, G. D., Redfern, S. A. T., Rhodes, N., Ross, N. L., Schofield, P. F., Schooneveld, E., Syfosse, G., Tucker, M. G. & Welch, M. D. (2001). *Neutron diffraction at simultaneous high temperatures and pressures, with measurement of temperature by neutron radiography. Min. Mag*. **65**, 749–760.
Le Godec, Y., Dove, M. T., Redfern, S. A. T., Marshall, W. G., Tucker, M. G., Syfosse, G. & Besson, J. M. (2002). *A new high P–T cell for neutron diffraction up to 7 GPa and 2000 K with measurement of temperature by neutron radiography. High Press. Res.* **65**, 737–748.
LeSar, R., Ekberg, S. A., Jones, L. H., Mills, R. L., Schwalbe, L. A. & Schiferl, D. (1979). *Raman spectroscopy of solid nitrogen up to 374 kbar. Solid State Commun.* **32**, 131–134.
Letoullec, R., Pinceaux, J. P. & Loubeyre, P. (1988). *The membrane diamond anvil cell: a new device for generating continuous pressure and temperature variations. High Press. Res*. **1**, 77–90.
Liebermann, R. C. (2011). *Multi-anvil, high pressure apparatus: a half-century of development and progress. High Press. Res*. **31**, 493–532.
Liu, Z. X., Cui, Q. L. & Zou, G. T. (1990). *Disappearance of the ruby R-line fluorescence under quasihydrostatic pressure and valid pressure range of ruby gauge. Phys. Lett. A*, **143**, 79–82.
McMahon, M. I. (2004). *High pressure diffraction from good powders, poor powders and poor single crystals.* In *High-Pressure Crystallography*, edited by A. Katrusiak & P. F. McMillan, pp. 1–20. Dordrecht: Kluwer.
McMahon, M. I. (2005). *Structures from powders and poor-quality single crystals at high pressure. J. Synchrotron Rad.* **12**, 549–553.
McMahon, M. I. (2012). *High-pressure crystallography. Top. Curr. Chem.* **315**, 69–109.
McWhan, D. B., Bloch, D. & Parisot, G. (1974). *Apparatus for neutron diffraction at high pressure. Rev. Sci. Instrum.* **45**, 643–646.
Malinowski, M. (1987). *A diamond-anvil high-pressure cell for X-ray diffraction on a single crystal. J. Appl. Cryst.* **20**, 379–382.
Mao, H. K. & Bell, P. M. (1979). *Observations of hydrogen at room temperature (25°C) and high pressure (to 500 kilobars). Science*, **203**, 1004–1006.
Mao, H. K., Bell, P. & Hadidiacos, C. (1987). *Experimental phase relations in iron to 360 kbar, 1400°C, determined in an internally heated diamond-anvil apparatus.* In *High-Pressure Research in Mineral Physics*, edited by M. H. Manghnani & Y. Syono, pp. 135–138. San Francisco: Terrapub/AGU.
Mao, H.-K., Bell, B. M., Shaner, J. W. & Steinberg, D. J. (1978). *Specific volume measurements of Cu, Mo, Pd, and Ag and calibration of the ruby R_1 fluorescence pressure gauge from 0.06 to 1 mbar. J. Appl. Phys.* **49**, 3276–3283.
Mao, H.-K., Chen, X.-J., Ding, Y., Li, B. & Wang, L. (2018). *Solids, liquids and gases under high pressure. Rev. Mod. Phys.* **90**, 015007.
Mao, H. K., Shu, J., Shen, G. Y., Hemley, R. J., Li, B. S. & Singh, A. K. (1998). *Elasticity and rheology of iron above 220 GPa and the nature of the Earth's inner core. Nature*, **396**, 741–743.
Mao, H.-K., Xu, J. & Bell, P. M. (1986). *Calibration of the ruby pressure gauge to 800 kbar under quasi-hydrostatic conditions. J. Geophys. Res.* **91**, 4673–4676.
Merlini, M., Crichton, W. A., Hanfland, M., Gemmi, M., Müller, H., Kupenko, I. & Dubrovinsky, L. (2012). *Structures of dolomite at ultrahigh pressure and their influence on the deep carbon cycle. Proc. Natl Acad. Sci. USA*, **109**, 13509–13514.
Merrill, L. & Bassett, W. A. (1974). *Miniature diamond anvil pressure cell for single crystal X-ray diffraction studies. Rev. Sci. Instrum.* **45**, 290–294.
Mezouar, M., Crichton, W. A., Bauchau, S., Thurel, F., Witsch, H., Torrecillas, F., Blattmann, G., Marion, P., Dabin, Y., Chavanne, J., Hignette, O., Morawe, C. & Borel, C. (2005). *Development of a new state-of-the-art beamline optimized for monochromatic single-crystal and powder X-ray diffraction under extreme conditions at the ESRF. J. Synchrotron Rad.* **12**, 659–664.
Miletich, R., Allan, D. R. & Kuhs, W. F. (2000). *High-pressure single crystal techniques. Rev. Mineral. Geochem.* **41**, 445–519.

Miletich, R., Cinato, D. & Johänntgen, S. (2009). *An internally heated composite gasket for diamond-anvil cells using the pressure chamber wall as the heating element. High Press. Res.* **29**, 290–305.

Mills, R. L., Liebenberg, D. H., Bronson, J. C. & Schmidt, L. C. (1980). *Procedure for loading diamond cells with high-pressure gas. Rev. Sci. Instrum.* **51**, 891–895.

Ming, L. C. & Bassett, W. A. (1974). *Laser heating in the diamond anvil press up to 2000˚C sustained and 3000˚C pulsed at pressures up to 260 kilobars. Rev. Sci. Instrum.* **45**, 1115–1118.

Moore, M. J., Sorensen, D. B. & DeVries, R. C. (1970). *A simple heating device for diamond anvil high pressure cells. Rev. Sci. Instrum.* **41**, 1665–1666.

Murata, K., Yokogawa, K., Yoshino, H., Klotz, S., Munsch, P., Irizawa, A., Nishiyama, M., Iizuka, K., Nanba, T., Okada, T., Shiraga, Y. & Aoyama, S. (2008). *Pressure transmitting medium Daphne 7474 solidifying at 3.7 GPa at room temperature. Rev. Sci. Instrum.* **79**, 085101.

Nelmes, R. J. & McMahon, M. I. (1994). *High-pressure powder diffraction on synchrotron sources. J. Synchrotron Rad.* **1**, 69–73.

Oehzelt, M., Weinmeier, K., Heimel, G., Pusching, P., Resel, R., Ambrosch-Draxl, C., Porsch, F. & Nakayama, A. (2002). *Structural properties of anthracene under high pressure. High Press. Res*. **22**, 343–347.

Okuchi, T., Sasaki, S., Ohno, Y., Abe, J., Arima, H., Osakabe, T., Hattori, T., Sano-Furukawa, A., Komatsu, K., Kagi, H., Utsumi, W., Harjo, S., Ito, T. & Aizawa, K. (2012). *Neutron powder diffraction of small-volume samples at high pressure using compact opposed-anvil cells and focused beam. J. Phys. Conf. Ser.* **377**, 012013.

Olejniczak, A. & Katrusiak, A. (2010). *Pressure induced transformations of 1,4-diazabicyclo[2.2.2]octane (dabco) hydroiodide: diprotonation of dabco, its N-methylation and co-crystallization with methanol. CrystEngComm*, **12**, 2528–2532.

Olejniczak, A. & Katrusiak, A. (2011). *Pressure-induced hydration of 1,4-diazabicyclo[2.2.2]octane hydroiodide (dabcoHI). Cryst. Growth Des.* **11**, 2250–2256.

Onodera, A. (1987). *Octahedral-anvil high-pressure press. High Temp. High Press.* **19**, 579–609.

Onodera, A. & Amita, F. (1991). *Apparatus and operation.* In *Organic Synthesis at High Pressures*, edited by K. Matsumoto & R. M. Acheson. Chichester: John Wiley & Sons.

Palasyuk, T., Figiel, H. & Tkacz, M. (2004). *High pressure studies of $GdMn_2$ and its hydrides. J. Alloys Compd.* **375**, 62–66.

Palasyuk, T. & Tkacz, M. (2007). *Pressure-induced structural phase transition in rare earth trihydrides. Part II. SmH_3 and compressibility systematics. Solid State Commun*. **141**, 5, 302–305.

Paliwoda, D. K., Dziubek, K. F. & Katrusiak, A. (2012). *Imidazole hidden polar phase. Cryst. Growth Des.* **12**, 4302–4305.

Patyk, E., Skumiel, J., Podsiadło, M. & Katrusiak, A. (2012). *High-pressure (+)-sucrose polymorph. Angew. Chem. Int. Ed.* **51**, 2146–2150.

Piermarini, G. J. (2001). *High pressure X-ray crystallography with the diamond cell at NIST/NBS. J. Res. Natl Inst. Stand. Technol.* **106**, 889–920.

Piermarini, G. J., Block, S. & Barnett, J. D. (1973). *Hydrostatic limits in liquids and solids to 100 kbar. J. Appl. Phys.* **44**, 5377–5382.

Piermarini, G. J., Block, S., Barnett, J. D. & Forman, R. A. (1975). *Calibration of the pressure dependence of the R_1 ruby fluorescence line to 195 kbar. J. Appl. Phys.* **46**, 2774–2780.

Piermarini, G. J., Mighell, A. D., Weir, C. E. & Block, S. (1969). *Crystal structure of benzene II at 25 kilobars. Science*, **165**, 1250–1255.

Podsiadło, M. & Katrusiak, A. (2008). *Isostructural relations in dihalomethanes and disproportionation of bromoiodomethane. CrystEngComm*, **10**, 1436–1442.

Półrolniczak, A., Sobczak, S. & Katrusiak, A. (2018). *Solid-state associative reactions and the coordination compression mechanism. Inorg. Chem.* **57**, 8942–8950.

Ragan, D. D., Clarke, D. R. & Schiferl, D. (1996). *Silicone fluid as a high-pressure medium in diamond anvil cells. Rev. Sci. Instrum.* **67**, 494–496.

Redfern, S. A. T. (2002). *Neutron powder diffraction of minerals at high pressures and temperatures: some recent technical developments and scientific applications. Eur. J. Mineral*. **14**, 251–261.

Rivers, M., Prakapenka, V. B., Kubo, A., Pullins, C., Holl, Ch. M. & Jacobsen, S. D. (2008). *The COMPRES/GSECARS gas-loading system for diamond anvil cells at the Advanced Photon Source. High Press. Res.* **28**, 273–292.

Royer, C. A. (2002). *Revisiting volume changes in pressure-induced protein unfolding. Biochim. Biophys. Acta*, **1595**, 201–209.

Runowski, M., Marciniak, J., Grzyb. T., Przybylska, D., Shyichuk, A., Barszcz, B., Katrusiak, A. & Lis, S. (2017). *Lifetime nanomanometry – high-pressure luminescence of up-converting lathanide nanocrystals – $SrF_2:Yb^{3+},Er^{3+}$. Nanoscale*, **9**, 16030–16037.

Sakai, T., Yagi, T., Irifune, T., Kadobayashi, H., Hirao, N., Kunimoto, T., Ohfuji, H., Kawagushi-Imada, S., Ohishi, Y., Tateno, Sh. & Hirose, K. (2018). *High pressure generation using double-stage diamond anvil technique: problems and equations of state of rhenium. High Press. Res.* **38**, 107–119.

Sakai, T., Yagi, T., Ohfuji, H., Irifune, T., Ohishi, Y., Hirao, N., Suzuki, Y., Kuroda, Y., Asakawa, T. & Kanemura, T. (2015). *High-pressure generation using double stage micro-paired diamond anvils shaped by focused ion beam. Rev. Sci. Instrum.* **86**, 033905.

Samara, G. A., Hansen, L. V., Assink, R. A., Morosin, B., Schirber, J. E. & Loy, D. (1993). *Effects of pressure and ambient species on the orientational ordering in solid C_{60}. Phys. Rev. B*, **47**, 4756–4764.

Senyshyn, A., Engel, J. M., Oswald, I. D. H., Vasylechko, L. & Berkowski, M. (2009). *Powder diffraction studies of pressure-induced instabilities in orthorhombic $LnGaO_3$. Z. Kristallogr. Suppl.* **30**, 341–346.

Shen, G., Mao, H. K. & Hemley, R. J. (1996). *Laser-heated diamond anvil cell technique: double-sided heating with multimode Nd:YAG laser. Proceedings of the 3rd NIRIM International Symposium on Advanced Materials, ISAM'96*, 4–8 March 1996, Tsukuba, Japan, pp. 149–152. Tsukuba: National Institute for Research in Inorganic Materials.

Shen, Y., Kumar, R. S., Pravica, M. & Nicol, M. F. (2004). *Characteristics of silicone fluid as a pressure transmitting medium in diamond anvil cells. Rev. Sci. Instrum.* **75**, 4450–4454.

Sikora, M. & Katrusiak, A. (2013). *Pressure-controlled neutral–ionic transition and disordering of NH···N hydrogen bonds in pyrazole. J. Phys. Chem. C*, **117**, 10661–10668.

Singh, A. K. (1993). *The lattice strains in a specimen (cubic system) compressed nonhydrostatically in an opposed anvil device. J. Appl. Phys.* **73**, 4278–4286.

Singh, A. K. & Balasingh, C. (1994). *The lattice strains in a specimen (hexagonal system) compressed nonhydrostatically in an opposed anvil high pressure setup. J. Appl. Phys.* **75**, 4956–4962.

Singh, A. K., Balasingh, C., Mao, H. K., Hemley, R. J. & Shu, J. (1998). *Analysis of lattice strains measured under nonhydrostatic pressure. J. Appl. Phys.* **83**, 7567–7575.

Smith, R. F., Eggert, J. H., Jeanloz, R., Duffy, T. S., Braun, D. G., Patterson, J. R., Rudd, R. E., Biener, J., Lazicki, A. E., Hamza, A. V., Wang, J., Braun, T., Benedict, L. X., Celliers, P. M. & Collins G. W. (2014). *Ramp compression of diamond to five terapascals. Nature*, **511**, 330–333.

So, P. T. C., Gruner, S. M. & Shyamsunder, E. (1992). *Automated pressure and temperature control apparatus for X-ray powder diffraction studies. Rev. Sci. Instrum.* **63**, 1763–1770.

Sobczak, S., Drożdż, W., Lampronti, G. I., Belenguer, A. M., Katrusiak, A. & Stefankiewicz, A. R. (2018). *Dynamic covalent chemistry under high pressure: a new route to disulfide metathesis. Chem. Eur. J.* **24**, 8769–8773.

Srinivasa, S. R., Cartz, L., Jorgensen, J. D., Worlton, T. G., Beyerlein, R. A. & Billy, M. (1977). *High-pressure neutron diffraction study of Si_2N_2O. J. Appl. Cryst.* **10**, 167–171.

Stishov, S. M. & Popova, S. V. (1961*a*). *New dense polymorphic modification of silica. Geokhimiya*, **10**, 837–839.

Stishov, S. M. & Popova, S. V. (1961*b*). *New dense polymorphic modification of silica. Geochemistry*, **10**, 923–926.

Syassen, K. (2008). *Ruby under pressure. High Press. Res.* **28**, 75–126.

Takahashi, H., Mori, N., Matsumoto, T., Kamiyama, T. & Asano, H. (1996). *Neutron powder diffraction studies at high pressure using a pulsed neutron source. High Press. Res*. **14**, 295–302.

Takahashi, E., Yamada, H. & Ito, E. (1982). *An ultrahigh-pressure furnace assembly to 100 kbar and 1500˚C with minimum temperature uncertainty. Geophys. Res. Lett.* **9**, 805–807.

Tateiwa, N. & Haga, Y. (2010). *Appropriate pressure-transmitting media for cryogenic experiment in the diamond anvil cell up to 10 GPa. J. Phys. Conf. Ser.* **215**, 012178.

Tkacz, M. (1995). *Novel high-pressure technique for loading diamond anvil cell with hydrogen. Pol. J. Chem.* **69**, 1205.

Tkacz, M. (1998). *High pressure studies of the rhodium–hydrogen system in diamond anvil cell. J. Chem. Phys.* **108**, 2084–2087.

Tomkowiak, H., Olejniczak, A. & Katrusiak, A. (2013). *Pressure-dependent formation and decomposition of thiourea hydrates. Cryst. Growth Des.* **13**, 121–125.

Van Valkenburg, A. (1962). *Visual observations of high pressure transitions. Rev. Sci. Instrum.* **33**, 1462.

Van Valkenburg, A., Mao, H.-K. & Bell, P. M. (1971*a*). *Solubility of minerals at high water pressures. Carnegie Inst. Washington Yearb.* **70**, 233–237.

Van Valkenburg, A., Mao, H.-K. & Bell, P. M. (1971*b*). *Ikaite ($CaCO_3$·6H_2O), a phase more stable than calcite and aragonite ($CaCO_3$) at high water pressure. Carnegie Inst. Washington Yearb.* **70**, 237–238.

Vereshchagin, L. F., Kabalkina, S. S. & Evdokimova, V. V. (1958). *Kamera dlya rentgenostrukturnykh issledovanii monokristallov pod vysokim davleniem. (A camera for X-ray diffraction studies of single crystals at high pressure). Prib. Tekh. Eksp.* **3**, 90–92.

Vos, W. L. & Schouten, J. A. (1991). *On the temperature correction to the ruby pressure scale. J. Appl. Phys.* **69**, 6744–6746.

Wang, J., Coppari, F., Smith, R. F., Eggert, J. H., Lazicki, A. E., Fratanduono, D. E., Rygg, J. R., Boehly, T. R., Collins, G. W. & Duffy, T. S. (2016). *X-ray diffraction of molybdenum under ramp compression to 1 TPa. Phys. Rev. B*, **94**, 104102.

Wartmann, E. (1859). *On the effect of pressure on the electric conductibility of metallic wires. Philos. Mag.* **17**, 441–442.

Wicks, J. K., Smith, R. F., Fratanduono, D. E., Coppari, F., Kraus, R. G., Newman, M. G., Rygg, J. R., Eggert, J. H. & Duffy, T. S. (2018). *Crystal structure and equation of state of Fe–Si alloys at super-Earth core conditions. Sci. Adv.* **4**, eaao5864.

Weir, C. E., Lippincott, E. R., Van Valkenburg, A. & Bunting, N. E. (1959). *Infrared studies in the 1–15-micron region to 30,000 atmospheres. J. Res. Natl Bur. Stand. USA*, **63A**, 5–62.

Whitfield, P. S., Nawaby, A. V., Blak, B. & Ross, J. (2008). *Modified design and use of a high-pressure environmental stage for laboratory X-ray powder diffractometers. J. Appl. Cryst.* **41**, 350–355.

Worlton, T. G. & Decker, D. L. (1968). *Neutron diffraction study of the magnetic structure of hematite to 41 kbar. Phys. Rev.* **171**, 596–599.

Xia, H., Duclos, S. J., Ruoff, A. L. & Vohra, Y. K. (1990). *New high-pressure phase transition in zirconium metal. Phys. Rev. Lett.* **64**, 204–207.

Xu, J., Mao, H. K., Hemley, R. J. & Hines, E. (2004). *Large volume high-pressure cell with supported moissanite anvils. Rev. Sci. Instrum.* **75**, 1034–1038.

Yagi, T., Yusa, H. & Yamakata, M. (1996). *An apparatus to load gaseous materials to the diamond-anvil cell. Rev. Sci. Instrum.* **67**, 2981–2984.

Yamaoka, H., Zekko, Y., Jarrige, I., Lin, J.-F., Hiraoka N., Ishii, H., Tsuei, K. D. & Mizuki, J. (2012). *Ruby pressure scale in a low-temperature diamond anvil cell. J. Appl. Phys.* **112**, 124503.

Yokogawa, K., Murata, K., Yoshino, H. & Aoyama, Sh. (2007). *Solidification of high-pressure medium Daphne 7373. Jpn. J. Appl. Phys.* **46**, 3636–3639.

You, Sh.-J., Chen, L.-Ch. & Jin, Ch.-Q. (2009). *Hydrostaticity of pressure media in diamond anvil cells. Chin. Phys. Lett.* **26**, 096202.

Zha, C. S. & Bassett, W. A. (2003). *Internal resistive heating in diamond anvil cell for in situ X-ray diffraction and Raman scattering. Rev. Sci. Instrum.* **74**, 1255–1262.

Zhao, Y. S., Lawson, A. C., Zhang, J. Z., Bennett, B. I. & Von Dreele, R. B. (2000). *Thermoelastic equation of state of molybdenum. Phys. Rev. B*, **62**, 8766–8776.

Zhao, Y. S., Von Dreele, R. B. & Morgan, J. G. (1999). *A high P–T cell assembly for neutron diffraction up to 10 GPa and 1500 K. High Press. Res.* **16**, 161–177.